UNITED NATIONS
UNIVERSITY
UNU-GTP
Geothermal Training Programme

Orkustofnun, Grensasvegur 9,
IS-108 Reykjavik, Iceland

Reports 2015
Number 10

SUBSURFACE GEOLOGY AND HYDROTHERMAL ALTERATION OF CACHAÇOS-LOMBADAS SECTOR, RIBEIRA GRANDE GEOTHERMAL FIELD, SÃO MIGUEL ISLAND, AZORES

António Franco
EDA RENOVÁVEIS
Rua Francisco Pereira Ataíde, 1
9504-535 Ponta Delgada, Acores
PORTUGAL
antonio.l.franco@eda.pt

ABSTRACT

The present report focuses on the high temperature geothermal area of Cachaços-Lombadas in the 245°C two-phase liquid dominated Ribeira Grande geothermal system in São Miguel Island. Subsurface geology and hydrothermal alteration are studied, using data from four of the eight existing wells. Emphasis is laid on the determination of the lithostratigraphy and identification of possible correlations between the geological units and the permeability encountered in the wells, including the analysis of tectonic structures inferred in the area. The present work reveals that pyroclastic rocks dominate the upper part of the subsurface geology, locally interrupted by trachyte lava flows and, at deeper levels, basalt lavas are the predominant lithological unit. Furthermore, the results show that north-northwestern trending structures probably play a very important role in the distribution of permeability in the Cachaços-Lombadas area.

Temperature distribution in the area was also investigated and the results are consistent with the main conclusions from previous studies, showing a clear boundary of the geothermal system in the southern part of the area and suggesting that the location of the upflow zone of the geothermal system is likely to be in the east to northeastern parts of the Cachaços-Lombadas area.

The alteration mineralogy allowed determining the alteration zoning pattern in the Cachaços-Lombadas area, identifying two zones of hydrothermal alteration, smectite zone and chlorite zone, beneath a shallow zone of relatively unaltered rocks. The hydrothermal alteration investigations were complemented with the study of fluid inclusions, allowing determination of the thermal history of the geothermal system. The results reveal that the geothermal system was hotter at some point in the past. However, since cooling has occurred, the system has been in equilibrium, with evidence of some fluctuations of the fluid levels within the geothermal reservoir.

1. INTRODUCTION

1.1 Geographical location of the Azores

The Azores Archipelago is a group of nine islands located in the middle of the Atlantic Ocean (Figure 1), 1600 km away from Portugal and 3800 km from the east coast of the USA. The population is approximately 240,000 inhabitants and of those about two thirds live on the largest island, São Miguel. The islands are spread along 600 km and, because of that, each island must be energy self-sufficient. Thus, the very small energy market, associated with the remote and isolated location of the region make the energy projects less attractive to private investors and, therefore, geothermal development must be publically driven (Rangel et al., 2011).

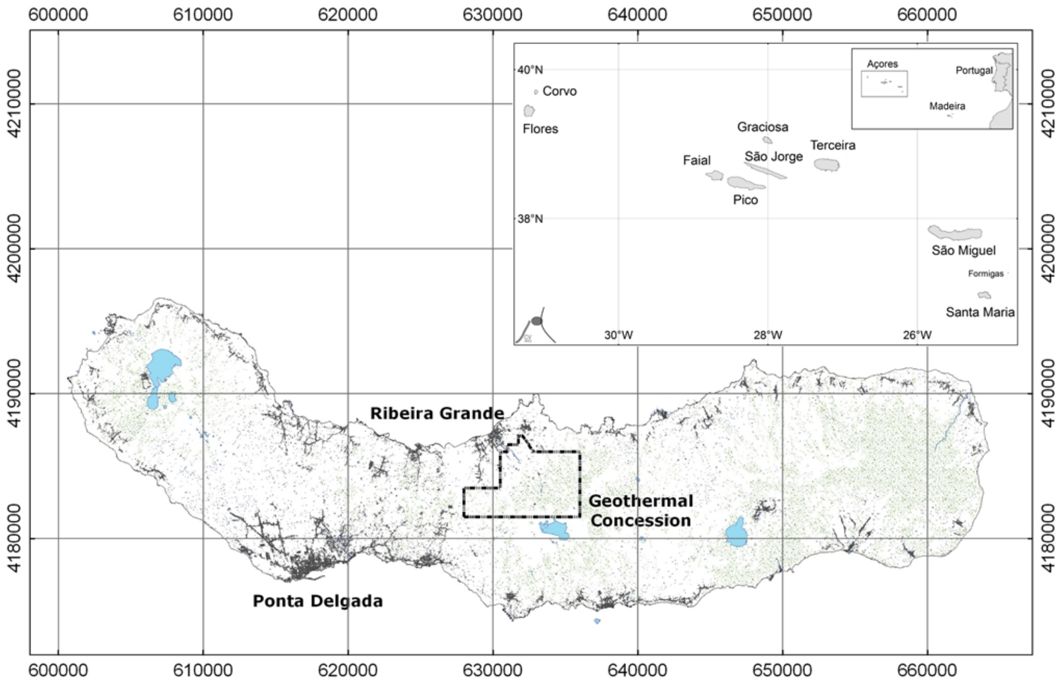

FIGURE 1: Geographical location of São Miguel Island, showing the location of Ribeira Grande geothermal concession (map provided by EDA RENOVÁVEIS)

1.2 History of geothermal projects in the Azores

Geothermal exploration in São Miguel Island started in 1976, with the execution of geophysical surveys (geoelectric and magnetotelluric), which identified a resistivity anomaly in the northern flank of Fogo volcano (Figure 2) which is possibly related to the presence of a geothermal system. This exploration was spurred by the findings in 1973 when a well was drilled to 981 m depth close to the city of Ribeira Grande (Figure 2) and encountered steam productive zones and temperatures exceeding 200°C (Muecke et al., 1974). This well was part of the ''Deep Drill'' project, developed by scientists at Dalhousie University and Lamont-Doherty Geological Observatory, and was planned to enhance the understanding of the structure, petrology and geochemistry of oceanic islands (Muecke et al., 1974).

In 1973, six thermogradient wells were drilled to 200 m depth and confirmed the existence of an extensive temperature anomaly in the northern flank of the Fogo volcano. These were followed by drilling of five exploratory wells (RG1, RG2, PV1, PV2 and SB1) from 1978 to 1981 which confirmed the existence of a high temperature geothermal reservoir (Hennerberger and Nunes, 1990), finding temperatures up to 230-235°C at -150 to -200 m mean sea level (m.s.l.).

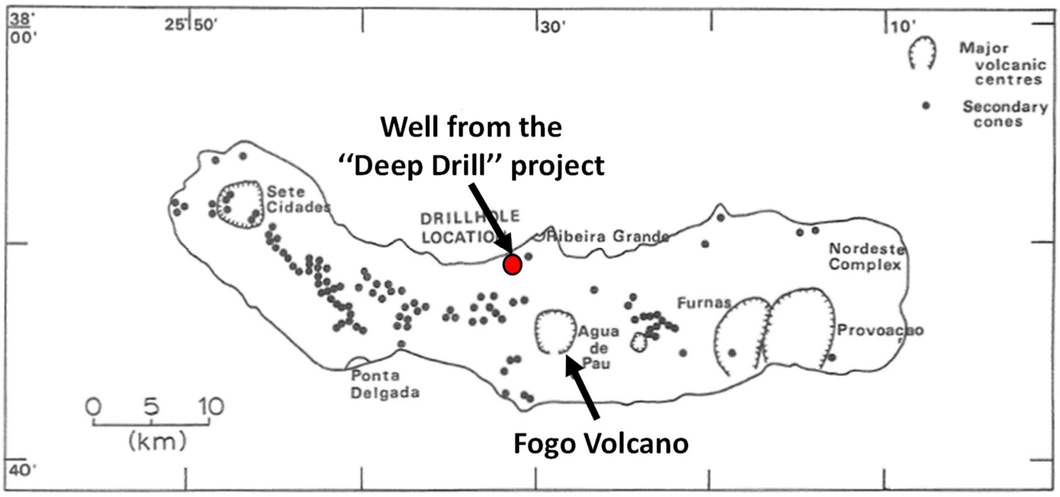

FIGURE 2: Location of the well drilled in the scope of the "Deep Drill" project (adapted from McGraw, 1976)

PV1 led to the installation of a small 3 MW geothermal pilot power plant, flash type, with a backpressure turbine which operated from 1980 to 2005 (Ponte, 2012). This project represented the first milestone of geothermal power production in the Azores and it was a very important breakthrough for the geothermal project because the pilot plant acted as a school for the technical staff who learned how to operate the industrial equipment and allowed to enhance the knowledge of the geothermal resource.

From 1989 to 1994, four wells (CL1, CL2, CL3, and CL4) were drilled in the southern part of the geothermal field, at higher elevations on the Fogo volcano and production of these wells was more than sufficient to supply Phase A of the Ribeira Grande plant (5 MW organic binary cycle) (Granados et al, 2000). The power plant went online in 1994, starting the industrial geothermal power production in the Azores. The wells were relatively prolific and the power plant was later expanded to 13 MW in 1999. During the past twenty-five years, three make-up wells were drilled for additional fluid supply to the power plant in order to maintain the load factor at high levels. This was the case for wells CL5 (2000), CL6 (2005) and CL7 (2010). More recently, well CL4-A was drilled in 2012 to serve, in combination with CL4, the reinjection of the effluent (brine and steam condensate) from the power plant, returning it back into the geothermal reservoir.

Meanwhile, in 2005, the pilot power plant at Pico Vermelho was dismantled and a new 10 MW power plant was installed in the same area (Cabecas et al., 2010) after the drilling of 6 additional wells was completed (PV3, PV4, PV5, PV6 and PV7 and PV8). This power plant was online by the end of 2006. Since then, it has achieved consistent production results with high availability (> 99%) and high load factor (> 99%) (Rangel et al., 2011). Within the first year in operation, numerical modelling studies had shown the possibility of thermal breakthrough within the reservoir due to reinjection in wells PV5 and PV6 (Ponte et al., 2010). Therefore, three new injection wells (PV9, PV10 and PV11) were drilled in 2009 and reinjection of brine and steam condensate from Pico Vermelho power plant is now being employed in these wells.

Since 1990, the geothermal development was driven by SOGEO (Sociedade Geotérmica dos Acores, S. A.), following the work of previous regional government institutions (Rangel et al., 2011). Meanwhile, in 2014, SOGEO merged with the EEG (Electricidade e Gás, S.A.), the company that exploits hydro and wind resources, and changed its denomination to EDA RENOVÁVEIS. In 2014, the geothermal contribution to total generation reached an average of 44% in São Miguel Island, representing about 23% of the overall power produced in the Azores (EDA, 2014). Therefore, the geothermal project of the Azores provides a significant contribution to the energy self-sufficiency of this remote and isolated region, offering clean, secure and cost-competitive energy, diminishing the needs for the use of fossil fuels.

2. OBJECTIVES

This work aimed at investigating the subsurface geology and hydrothermal alteration in the Ribeira Grande geothermal field, focusing on the Cachaços-Lombadas sector, located in the southern part of the field, and possibly providing some valuable information regarding what to expect in future wells to be drilled within this area. The main objectives of the study are described below:

- Establishing a correlation between the geological formations intersected by the geothermal wells and, if possible, try to identify the transition from subaerial to submarine deposits (phreatic breccias);
- Determining if there is any consistent relation between the geology and the permeability of the reservoir;
- Making a first determination of the alteration zone and determine the thermal evolution of the geothermal system, namely, weather if it is in equilibrium, heating or cooling.

3. GEOLOGICAL BACKGROUND

3.1 Tectonic setting of the Azores and the Fogo volcano

The Azores Islands are located on the triple-junction of the Azores where the Eurasian, African and American tectonic plates meet. As Figure 3 shows, the nine islands of the Archipelago are divided into three groups with Flores and Corvo located on the North American plate whilst the eastern (São Miguel and Santa Maria islands) and the central group (Faial, Pico, São Jorge and Terceira islands) are located along the Terceira Rift which corresponds to the western segment of the Azores-Gibraltar fault zone. The islands from the eastern and central groups follow a WNW-ESE trend and emerge above the sea in the Azores Plateau which is defined by the bathymetric line of 2000 m (Rangel et al., 2011) and marks the transition to the nearby abyssal planes with depths of over 3500 m.

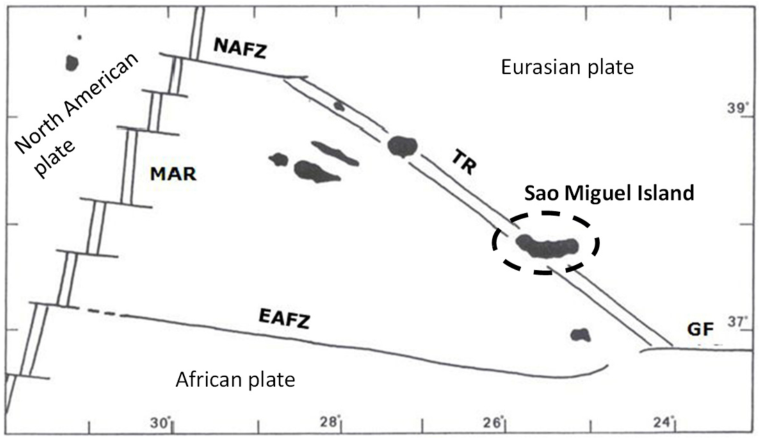

FIGURE 3: Main tectonic structures in the Azores region: MAR – Mid Atlantic Ridge; NAFZ – Northern Azores Fault Zone; EAFZ – Eastern Azores Fault Zone; TR – Terceira Rift; GF – Glória Fault (adapted from Gaspar, 1996)

According to Carmo (2013), the fault pattern in the Azores is characterized by two main fault systems with oblique slip, each of which is composed of two sets dipping in opposite directions: WNW-ESE to NW-SE normal dextral faults and conjugated NNW-SSE to N-S normal lateral structures. With this arrangement, the fault pattern exhibits a horizontal maximum compressive stress trending NW-SE (σ1), a horizontal minimum compressive axis trending NE-SW (σ3) and a vertical intermediate compressive stress axis (σ2). The resultant deformation is accommodated by several active faults where significant volcanic and seismic activity occurs.

São Miguel Island is located near the southeast end of the Terceira Rift and its most important tectonic structures follow the general pattern of the Azores Plateau with main directions NW-SE and WNW-ESE

(Silva et al., 2011). Therefore, the island is characterized by significant seismicity associated with these NW-SE and WNW-ESE structures (Queiroz, 1997; Ferreira, 2000).

The most important tectonic structure of the Fogo volcano is the graben of Ribeira Grande (Figure 4). The identification of tectonic structures at the surface is somewhat difficult in the Fogo volcano, due to the fact that most of the faults are covered by thick layers of pyroclastic units or are obscured by dense vegetation. Therefore, most of the structures are inferred by lineaments formed by the volcanic structures and from the linear river streams/creeks.

According to Carmo (2013), the orientation of the main structures of Ribeira Grande graben is in agreement with the main direction of the regional tectonic stresses, associated with the Terceira Rift. The graben itself extends over most of the northern flank of the volcano and its limits are defined by two lineaments of volcanic peaks. The western limit is given by the fault zone of Ribeira Grande, a lineament with about 7 km in extension formed by Pico da Varanda, Pico da Madeira, Pico dos Carneiros, Pico Queimado and the scoria cone of Rochão. The eastern limit corresponds to the fault zone of Falca which is defined by a 9 km lineament formed by the volcanic peaks of Cintrão, Pico da Vinha, Lameiro, Coroa da Mata, Pico Redondo and Monte Escuro.

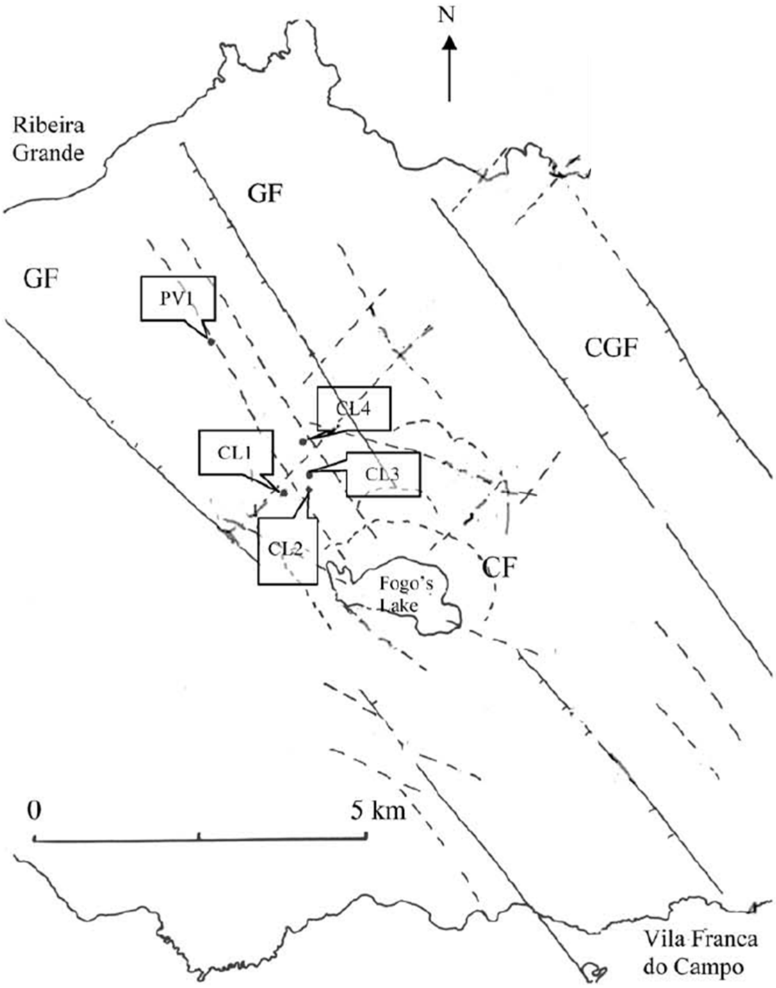

FIGURE 4: The graben of Ribeira Grande, showing the location of the geothermal wells (PV1, CL1, CL2, CL3 and CL4). GF denotes the Graben faults; CF denotes caldera faults; and CGF denotes Congro's fault system. Solid lines denote known faults, dashed lines inferred faults (modified from Carvalho et al., 2006)

As shown in Figure 4, the main structures observed in the graben of Ribeira Grande are NW-SE and NNW-SSE trending. The vertical displacement of the normal faults that limit the graben is uncertain because this tectonic valley has been filled with successive volcanic material from recent eruptions, such as the FOGO A unit, which can reach up to 20 m in thickness (Carmo, 2013). Furthermore, according to Muecke et al., (1974), based on the geological data collected from core samples in a well drilled in 1973 in the scope of the "Deep Drill" Project the graben of Ribeira Grande has suffered subsidence of about 650 m in the last 690,000 years. This was suggested by the appearance of submarine deposits at only about 700-800 m depth with the uppermost part of the well lithology consisting only of subaerial facies.

Moreover, the fact that there are no surface expressions of the normal fault zones that correspond to the boundaries of the graben suggests that volcanic activity and the rate of the material filling the graben exceeds the tectonic activity associated with the graben faults (Carmo, 2013).

3.2 Geology of Fogo volcano

Along with Sete Cidades and Furnas, Fogo is one of the three late Quaternary stratovolcanoes of São Miguel Island. Located in the central part of the island (Figure 5), Fogo is a central volcano with a summit about 900 meters above sea level, truncated by a 3 km wide caldera where the lake "Lagoa do Fogo" lies. Furthermore, the volcano morphology is characterized by an older outer caldera about 7x4 km across, which is preserved in the western, northern and eastern part of the volcano (Moore, 1991).

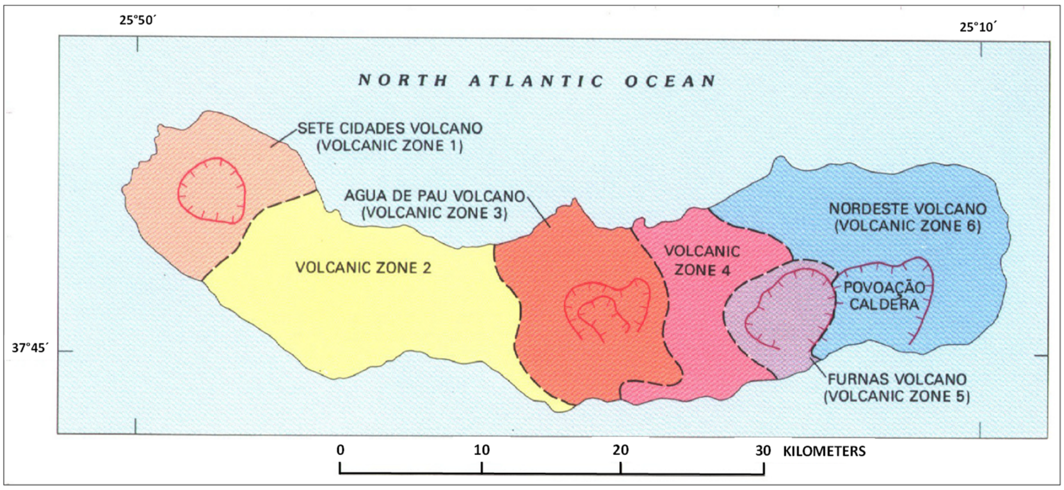

FIGURE 5: Location of Fogo volcano, identified as Agua de Pau volcano (Moore, 1991)

Inside the calderas there is only evidence of explosive activity, whereas several trachyte and mafic lava flows were erupted from vents located on the flanks of the volcano prior to and following the caldera formation (Moore, 1991). According to Booth et al. (1978), during the last 5,000 years at least five eruptions of trachyte pumice have occurred from vents located within the inner caldera.

The rock types show geochemical bimodality with the trachyte compositions dominating and the intermediate compositions representing a minor volumetric part of the eruptions. The lava flows and the pyroclastic deposits of the Fogo volcano are classified as alkali basalt-trachyte (Irvine and Barager, 1971).

As shown in Figure 6, the Fogo volcano stratigraphy can be divided into the following main units:

- *The Pleistocene units* correspond to the oldest subaerial rocks and according to Moore (1990), these include a trachyte dome (181,000 years old) on the southern flank, a trachyte flow (121,000 years old) near the summit and a trachyte welded tuff (103,000 years old) deposits on the northeast coast. The main edifice of the volcano was built around 40,000 to 100,000 years ago and it consists of trachyte lava flows, domes and pyroclastic deposits (Moore, 1990);
- *Older caldera – outflow deposit:* This corresponds to the collapse episodes of the summit caldera. Although this might have occurred several times, only two deposits show clear evidence of such episodes. These mostly correspond to several cubic meters of welded and non-welded pumice which can be found in outcrops on the north eastern and south eastern flanks of the volcano as well as exposures of welded tuff deposits on the northern and south eastern flanks of the volcano which can be seen filling the canyons near the margins of the early trachyte flows and overlying trachyte flows;
- *Post-outer caldera units:* There is no evidence for the occurrence of any eruptions within the outer caldera limits for about 15,000 to 30,000 years. Nevertheless, a few eruptions of tristanite and possibly mafic lavas occurred from vents located on the flanks of the volcano.
- *Younger caldera – outflow deposit:* The inner caldera was formed about 15.200 years ago as a result of a large Plinian eruption which produced large volumes of non-welded pumice and

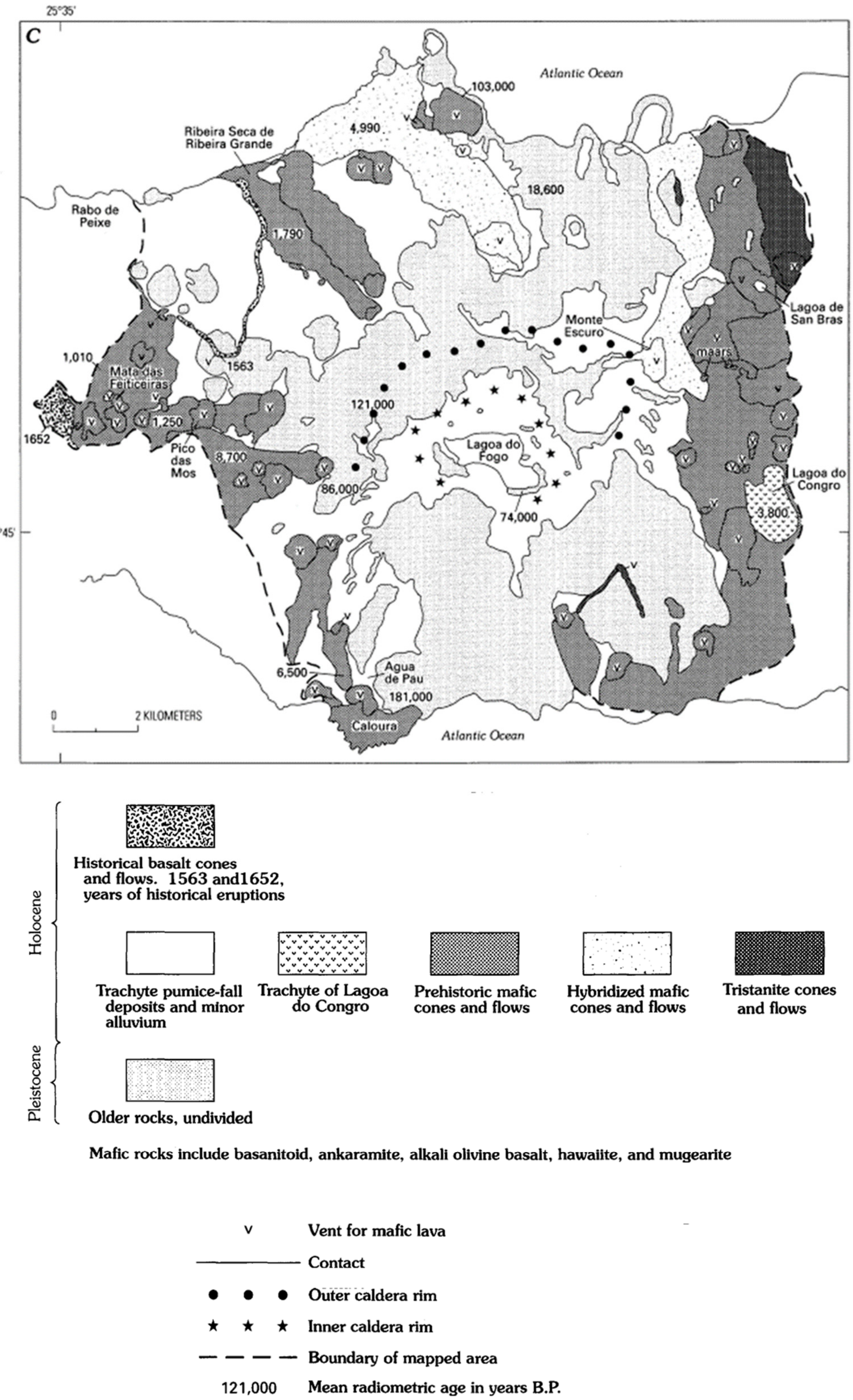

FIGURE 6: Geological map of Fogo volcano (Moore, 1991)

- locally welded pyroclastic flows. Exposures of these deposits can be found on the southern flank of the volcano with the best outcrops being located in the sea cliffs between Trinta Reis and Pisoes.
- *Post-inner caldera units*: According to Moore (1990), until about 10,000 years ago no important eruptions occurred within the inner caldera. Nevertheless, six trachyte domes and associated

flows were formed just outside the outer caldera rim on the western and north western flanks of the volcano.

- *Holocene units* are resulting mostly from the activity in the inner caldera about 5,000 years ago. These include the large Plinian fall deposit Fogo A which was probably formed in at least five separate eruptions (Moore, 1990) as well as other minor pyroclastic and mudflows (Walker and Crossdale, 1970). The Fogo A deposit is one of the most valuable chronostratigraphic marker beds because no other major trachytic eruption is known on central and eastern São Miguel at this time.

3.3 Historical eruptions and seismic activity

Due to its geodynamic setting, the Azores are frequently associated with seismic and volcanic activity. Since settlement in the 15th century, 30 earthquakes of tectonic origin were felt in the Azores, killing approximately 5000 people and causing significant damage (Carvalho et al., 2001). Some of these earthquakes are estimated to have reached magnitudes of up to 7 on the Richter scale. During this period, about 30 volcanic eruptions took place in the Azores, causing about 240 deaths. The last volcanic eruption was in 1998 and it was located in the sea, west of Terceira Island. The last major earthquake was felt in Faial in 1998, reaching a magnitude of 6 on the Richter scale (Carvalho et al., 2001).

The source of the volcanic activity in the Azores has been considered to be related to the presence of a mantle plume (Madureira et al., 2005, 2014) and the region is considered as a typical example of hot spot-ridge interaction but this has been under intense debate (Métrich et al., 2014). Since the settlement three volcanic eruptions have occurred in São Miguel Island, two in Furnas Volcano in 1439-43 and 1630 (Booth et al., 1978; Cole et al., 1995) and one in Fogo in 1563 (Figure 7) (Wallenstein et al., 2007).

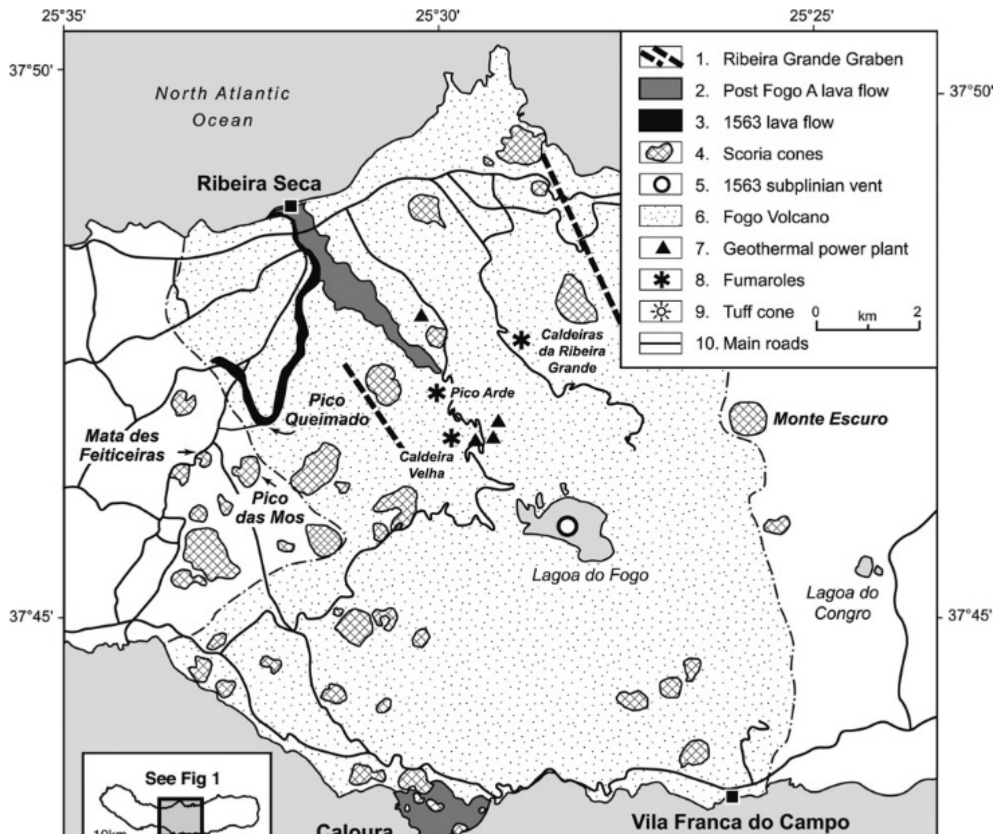

FIGURE 7: Volcanic structures and geothermal surface manifestations in the Fogo volcano, showing also the location of the 1563 eruptions (Wallenstein et al., 2007)

The 1563 eruption started as a Plinian eruption inside the inner caldera and, just a few days later, a Strombolian eruption started in a vent located in the north western flanks of the volcano (Pico Queimado) with the latter extruding a mafic lava flow that reached the villages of Ribeira Seca and Ribeira Grande located in the north coast of São Miguel Island (Figure 7).

At present time, the Fogo volcano is considered to be dormant. Several geothermal surface manifestations in the area include active fumarole fields, hot springs and soil diffuse degassing areas. As shown in Figure 7, these manifestations are mainly located in the northern flank of the Fogo volcano and are associated with NW-SE faults (Ferreira, 2000) with the main features being present at Pico Vermelho (near Pico Arde), Caldeira Velha and Caldeiras da Ribeira Grande.

Since the early 80´s, the seismic network of the Azores, operated by CIVISA (Centro de Informação e Vigilância Sismovulcânica dos Açores), has been monitoring the seismic activity of the Azores, registering hundreds of earthquakes and micro earthquakes. These data allowed delineating the major seismic areas of the Region. As shown in Figure 8, the seismic swarms are located along the Terceira Rift and on the Middle Atlantic Ridge and in their associated areas. This is the case of D. João de Castro submarine volcano, located between the Terceira and São Miguel islands or the seismic swarm located southeast from São Miguel Island. Additionally, it is important to note that seismicity in the region has been characterized by the occurrence of frequent low to moderate magnitude events, up to 2-3 on the Richter scale, but, as mentioned above, some strong earthquakes of magnitude 7 also occur.

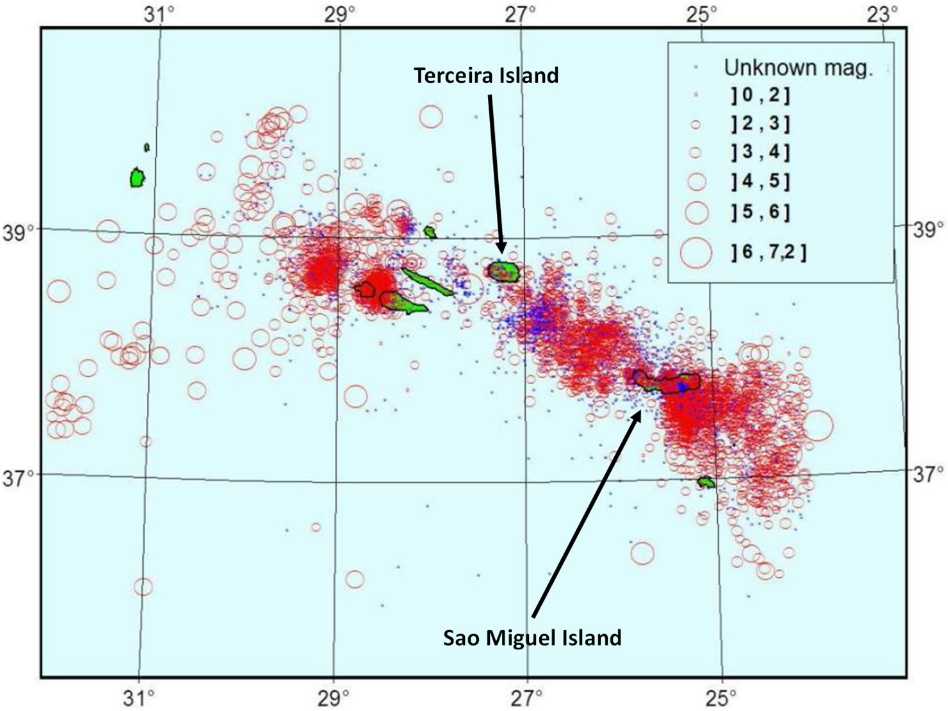

FIGURE 8: The Azores epicentral map for 1915 to 2011
(adapted from Rodrigues and Oliveira, 2013)

3.4 Ribeira Grande geothermal field

The main hydrothermal system of the Fogo volcano is located on the northern flank, associated with the northwest-southeast fault system corresponding to the graben of Ribeira Grande (Figure 4). The Ribeira Grande geothermal system is a high temperature system with temperatures up to 245°C, hosted by volcanic rocks, mainly pyroclastic units and lava flows. The system is elongated in a north-western direction and its boundaries probably follow the same strike (GeothermEx, 2008; Ponte et al., 2009).

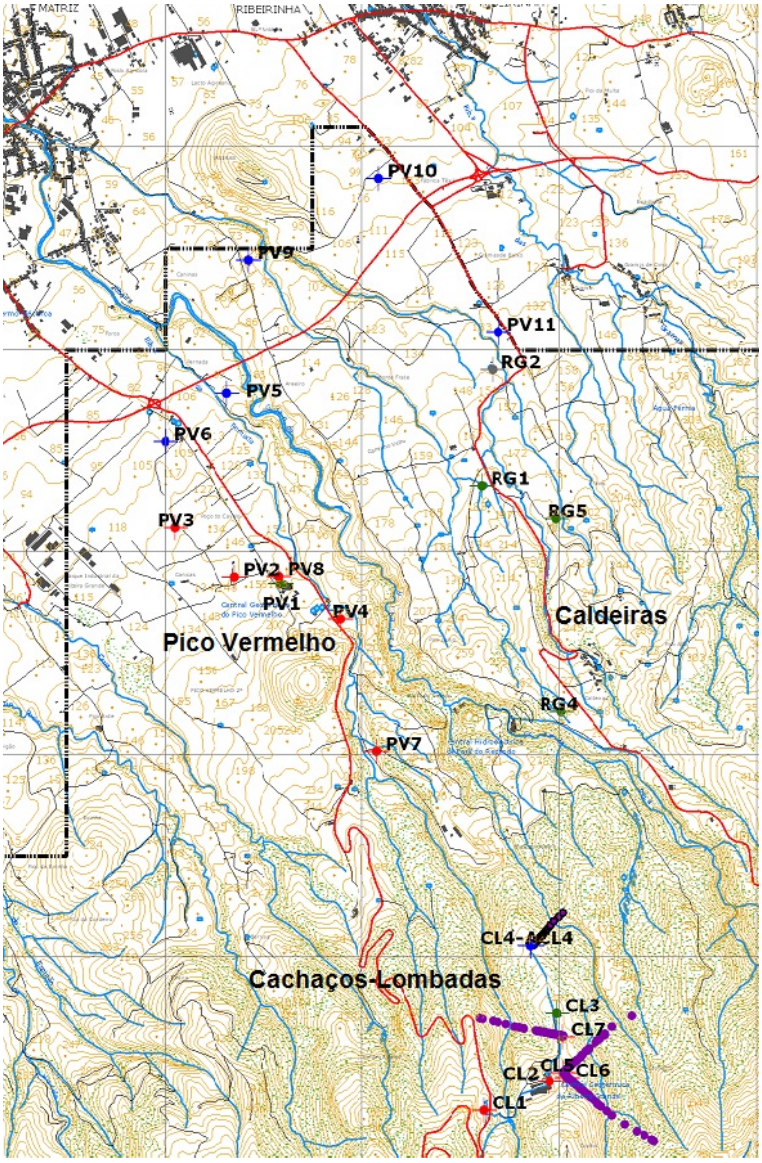

FIGURE 9: Location of the wells in the Ribeira Grande geothermal field (Rangel, 2014; provided by EDA RENOVÁVEIS)

The heat source is most likely related to a magmatic body or young intrusive rocks associated with the activity of the Fogo volcano (GeothermEx, 2008; Ponte et al., 2009; Pham et al., 2010; Ponte et al., 2010). In this respect, many studies have suggested that a trachytic magma chamber underlies the Fogo volcano (Booth et al., 1978; Duffield and Muffler, 1984; Gandido et al., 1984) and seismic studies undertaken by Dawson et al., (1985) indicated that the magma chamber is likely to be located at 10 to 12 km depth.

The subsurface geology and the geothermal reservoir conditions have been investigated by surface exploratory work and by drilling of shallow and deep geothermal wells. Based on the available data, the upflow to the geothermal system is located in the south eastern part of the geothermal field, probably east to northeast of wells CL3 and CL7 (Figure 9). The fluid subsequently moves upwards and northwestward, following the fault system of the Ribeira Grande graben and the outflow of the geothermal system which is likely towards the sea, in the northern part of the field (Figure 10) (GeothermEx, 2008; Ponte et al., 2009; Pham et al., 2010; Ponte et al., 2010).

The reservoir is two-phase and liquid dominated, the fluid composition being sodium-chloride type with total dissolved solids of 6 to 7 g/l and pH of 8-9. The chloride content is typically about 1500-1600 mg/l, the silica content ranges from 400 to 600 mg/l and the alkalinity is about 500 mg/l (Rangel et al., 2011). The permeability is mainly associated with fracture zones located within the basalt lava flows, likely to be associated with the northwest trending fault system of the Ribeira Grande graben. Furthermore, the fluid composition in the geothermal system is fairly homogeneous, indicating that good and well distributed permeability can be found in most of the field (GeothermEx, 2008). Additionally, oxygen and deuterium isotope analyses have shown that recharge of the geothermal system is of meteoric origin (Ponte et al., 2010; Rangel et al., 2011).

The cap rock of the geothermal system is composed of a sequence of pyroclastic units which are altered to clay, forming a relatively impermeable cap at the top of the reservoir. Because of the topography, the cap rock is found deeper in the wells located in the southern part of the field, namely at 500-650 m depth in the Cachaços-Lombadas sector (identified as Ribeira Grande area in Figure 10), whereas it is found at 300-400 m in the wells located further north in the Pico Vermelho sector.

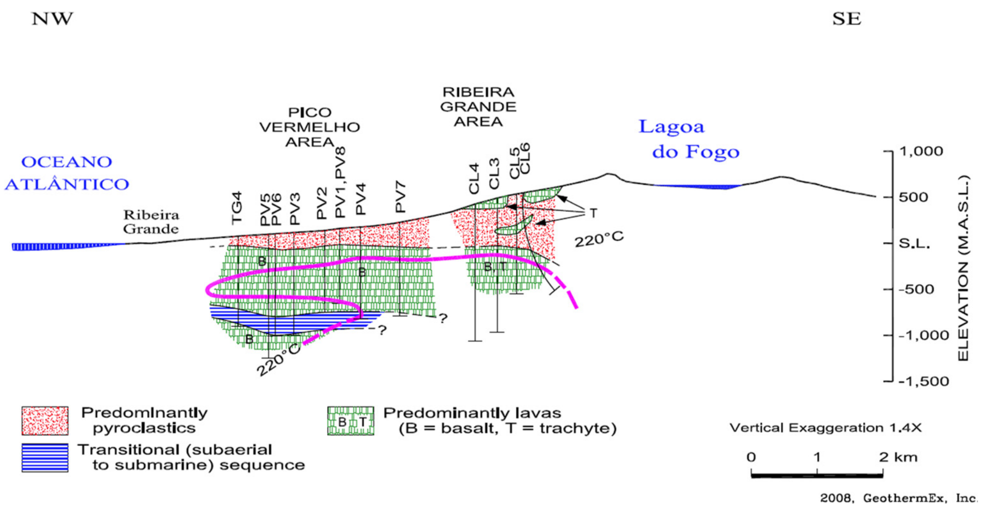

FIGURE 10: Generalized cross-section of the Ribeira Grande geothermal system (GeothermEx, 2008)

4. LITHOLOGY LOGS

All rocks intersected by the Cachaços-Lombadas wells are volcanic and correspond to the eruptive products of the Fogo volcano. The rock types include pyroclastic rocks, such as fine-grained tuffs and coarser tuffs with variable amounts of lithic fragments, pumice and crystals and different types of lavas, varying in composition from trachyte, basalt and intermediate. Based on binocular analyses of drill cuttings, the detailed descriptions of the lithological units and the stratigraphy of wells CL4-A, CL5, CL6 and CL7 is presented, respectively, in Appendices I and II. In summary, the different formations can be divided into three main units:

- *Pyroclastic rock units*. These incorporate all the glassy components (mostly ash and pumice) including tuffs, lithic tuffs with variable amounts of lava fragments, pumice and scoria, crystal rich tuffs and pumice deposits and they correspond to the predominant lithology in the uppermost part of the wells.
- *Crystalline trachyte lavas*. A shallow and relatively thick (up to 100-150 m thick) sequence of trachyte lavas is found near surface in five of the eight wells and it has very high secondary permeability. Below 200 m, at least three sequences of trachyte lavas can be identified and these are frequently found interspersed with the pyroclastic rock units. In general, the trachytes are massive, fine-grained with sugary appearance, commonly porphyritic with sparse sanidine phenocrysts.
- *Crystalline basalt lavas*. The darker lavas are more commonly found below sea level and form the predominant lithology in the reservoir interval. In general, the basalt flows are massive, fine-grained, with textures that vary from aphanitic to porphyritic with olivine and sparse pyroxene phenocrysts.

4.1 Correlation between the wells

4.1.1 Lithostratigraphic correlation

In the present study, drill cuttings from wells CL4-A, CL5, CL6, and CL7 were analysed jointly with previously acquired data on the lithology of the other wells in Cachaços-Lombadas area. In summary, the lithostratigraphy of the area can be described as follows:

- At shallow levels from the surface to about 250-300 m m.s.l., five wells intersect a thick sequence of trachyte lava. This is the case in CL1, CL2, CL3, CL4 and CL4-A. The sequence of trachyte lavas is absent in the wells CL5, CL6 and CL7, possibly because they thin out or are eroded away at these locations (Figure 11). It is important to note that this shallow sequence of trachyte lava is very permeable and caused severe losses of circulation fluid during drilling.
- A thick sequence of pyroclastic rocks is the predominant lithological unit from the surface to about -100 m m.s.l. At CL5, CL6, and CL7 it reaches about 600 m thickness, but is thinner in CL4-A where it is 300-400 m thick. This sequence of pyroclastic rocks underlies the sequence of trachyte lavas described above when the lavas are present. When the shallow trachyte lavas are not present, the pyroclastic rocks outcrop at the surface.
- The sequence of pyroclastic rocks, chiefly of trachytic character, is locally interrupted by lava flows of variable thickness which constitute a minor fraction of the total rock volume. These lava flows are mostly of trachyte composition, even though basalt and possibly intermediate types are present, too. Here, four sequences of lava give a good correlation between the wells in the area, namely two sequences of trachyte lava and two sequences of basalt lavas which are described below:
- The second sequence of trachyte lavas is found in about 240-160 m m.s.l., giving a good correlation between the wells CL6, CL5, and CL4-A. However, it is important to note that this intermediate-depth trachyte is thinner in CL7 than in CL5 and CL6 and the fact that this sequence of trachyte lava seems to thin out towards northwest could help explaining its absence in CL4-A. Additionally, the different depths of penetration into wells CL5 and CL6 indicates that this lavas dip north-westwards, which is consistent with the structure of the Fogo volcano;
- A third trachyte lava sequence is found at about 50-90 m m.s.l. It is thinner than the one described above but is present in all wells with the exception of CL5 where it possibly thins out;
- The first sequence of basalt lavas is found at about 100-200 m m.s.l. in wells CL4-A and CL7 but it only has a significant expression in well CL4-A where it is 90 m thick, whereas in CL7 this lava flow is very thin (4 m).
- A second sequence of basalt lavas is found at -30 to -60 m m.s.l. and there is a good correlation between wells CL5 and CL4-A. The second sequence of basalt lavas is not found in CL7 and keeping in mind that CL7 was drilled directionally towards NW, whereas CL5 and CL4-A were both drilled directionally towards NE, this could be related to the fact that these basalt lavas thin out towards NW.
- The pyroclastic rock units show a progressive increase of hydrothermal alteration with depth, particularly to clay minerals. This is consistent with the reduced permeability that is observed in the middle and at the bottom of the pyroclastic rock sequence. Here, secondary clays form the caprock of the geothermal system, limiting vertical flow and isolating the geothermal reservoir from the shallower groundwater.
- Below sea level and underlying the pyroclastic rock sequence, the subsurface geology is dominated by basalt lavas down up to about -600 m m.s.l. This is more prominent in CL4-A. Elsewhere, the extent of this of the lava dominated interval is rather uncertain, particularly in the area of wells CL6, CL5, and CL7 where this interval was drilled without returns. Low penetration rates while drilling in CL5 are consistent with the possibility that lavas are the predominant lithology in this interval. However, for wells CL6 and CL7 the rates of penetration did not show a major variation and cannot be used as a guide for estimation of the lithology types.
- No intrusive or subvolcanic rocks were identified in this study (except as clasts within pyroclastic deposits with the most commonly found being syenite). However, such rocks may occur at greater depths;
- The geological record from wells CL4-A, CL5, CL6, and CL7 did not allow the identification of the transition from subaerial to submarine deposits as no pillow lavas or phreatic breccias were observed in any of these wells. This observation is consistent with the high subsidence rate that the Ribeira Grande graben has suffered, as described in section 3.1 above, and to the fact that Cachaços-Lombadas wells are often drilled without returns below 600 m m.s.l.

4.1.2 Correlation between permeability and lithology

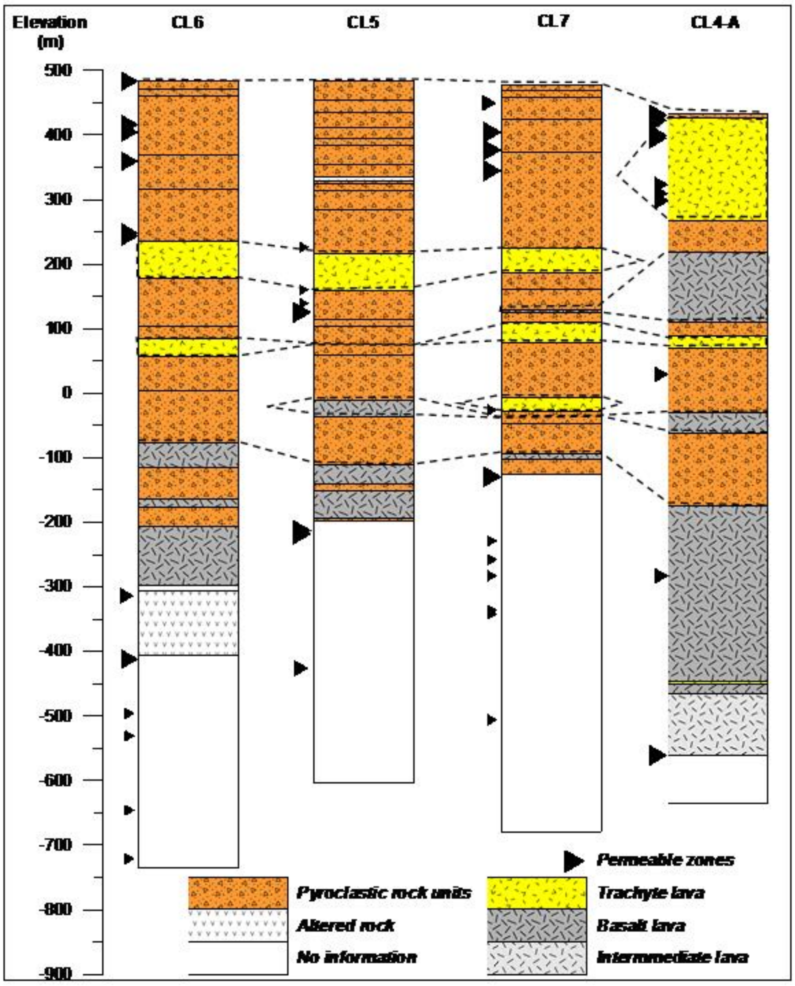

FIGURE 11: Schematic SE-NW lithology cross-section of Cachaços-Lombadas sector

Based on the drilling data, geological data and the temperature logs taken during heat recovery after completion of the wells, it was possible to identify the location of the permeable zones in CL4-A, CL5, CL6, and CL7. These are indicated in Figure 11 and in Appendix II. A summary of the distribution of permeability with depth is presented below.

The majority of the Cachaços-Lombadas wells, including CL4-A, intersect a shallow sequence of trachyte lava which is highly fractured and, therefore caused severe losses of circulation fluid during drilling. Wells CL5, CL6, and CL7 did not intersected this shallow sequence of trachyte lava but still significant permeable zones were found in these wells from about 500 to 350 m m.s.l., often related to zones of high porosity within the pyroclastic rock units or in the boundaries between units. Here, it is important to note that no significant permeable zones were reported in well CL5 at shallow depths because this well was drilled to 150 m using air-rated drilling, thus not allowing the identification of permeability with precision.

From 200 to -100 m m.s.l. permeability is very limited. Nevertheless, a few permeable zones were identified in CL5 and CL6 and these are mostly related to fracture zones within the trachyte lava flows or are located at their top and bottom boundaries.

Below -100 m m.s.l. the basaltic sequence predominates and marks the entry into reservoir conditions. Here, a zone of very high permeability is observed from -150 to -400 m, where frequently the fluid returns are lost during drilling of the wells. In most of the Cachaços-Lombadas wells, this is the zone were the most prolific feed zones are located. From there and down to about -700 m, the permeability is minor when compared to the zone above. The only exception to this was well CL4-A where a major permeable zone was found deeper at -561 m m.s.l.

4.1.3 Correlation between permeability and alteration minerals

Porosity and permeability are the primary factors that control movement and storage of fluids in the rock formations leading to the deposition of minerals, either in veinlets, veins or amygdales. In the Ribeira Grande geothermal field, some secondary minerals such as calcite, pyrite and silica phases (opal, chalcedony and quartz) are commonly found in or adjacent to aquifers, occurring as products of the alteration of the host rocks during water-rock interaction or as precipitates, filling open-spaces such as fractures, fissures or vesicles. Therefore, the occurrence and abundance of these minerals can serve as indicators of the presence of permeability.

A summary of the main findings from the comparison between the locations of the permeable zones against the abundance of the alteration minerals in the Cachaços-Lombadas wells is presented below:

- In CL4-A, pyrite abundance has good correlation to the permeability found in the well as the depths of the pyrite peaks found at 620 and 900-910 m have a good match to losses of circulation fluid during drilling (Appendix II). On the other hand, the distribution of calcite and silica minerals did not allow any correlation with the permeable zones found in the well. Calcite and silica appear at around 200-250 m depth and their abundance peaks at 300-320 m. A second peak is observed at about 420 m and then they become fairly common to the bottom of the well. However, during drilling, no significant permeable zones were seen here. Furthermore, where permeability was identified it is difficult to relate it to any specific abundant zone of calcite or silica, mostly because below 420 m and down to the depth of the last sample recovery these minerals are found in relatively high abundance;
- In CL5, the major permeable zone encountered at 710-715 m is just preceded by a peak in the silica and pyrite veining (Appendix II). Other peaks in the abundance of silica and pyrite are seen at 460-500 m and 540-620 m but no permeability was observed here, suggesting that the majority of the open-spaces within the rock formation were sealed by the precipitation of the secondary minerals.
- In CL6, the permeable zones are accompanied by peaks in the abundance of secondary minerals. As shown in Appendix II, the permeable zone at 260 m depth matches a peak of pyrite and the feed zones at 800 and 900 m are accompanied by vein peaks of the calcite, pyrite and quartz.
- In CL7, pyrite was found and it was fairly abundant at about 120-160 m depth, quite shallow in comparison to the other Cachaços-Lombadas wells (Appendix II). This pyrite peak corresponds to a zone of high permeability found in the well. Other pyrite peaks were found at 200-240 m, 300-340 m and 460-500 m and these were accompanied by calcite and silica peaks. However, no permeable zones were identified in these intervals, suggesting that permeability was present there at some point in the past but it is now sealed.

4.1.4 Relation between permeability and tectonic structures

The geological structure of the Ribeira Grande geothermal field is influenced by tectonic and volcanic stresses which combine to form a local pattern of faulting and fracturing. Regional tectonic stresses are associated with the triple junction of the Azores, more specifically with the Terceira Rift, whereas the local stresses are related to the Fogo volcano and its caldera faulting. The identification of tectonic structures applying common surface mapping techniques is rather difficult for the Fogo volcano because they are obscured by dense vegetation and are covered by thick pyroclastic rock units. Therefore, most of the structures mapped in the previous studies were inferred by topographic trends and lineaments from the volcanic structures. As described above in Section 3.1 and as shown in Figure 4, these lineaments indicate that over the entire Ribeira Grande geothermal field there is a predominant north-westward structural trend, associated with the graben of Ribeira Grande.

The lithological data from the wells, described in Section 4.1.1, does not allow for direct identification of any faults that might be present in the Cachaços-Lombadas area. The lava flows can be used locally as marker horizons, particularly the sequences of trachyte lavas that are intersected by the wells from 500 to about -100 m depth, but where they are present, the correlation between these marker horizons often indicates that the lava flows tend to dip towards north or northwest which is coincident with the structure of the Fogo volcano. Additionally, where there are significant vertical displacements between the depths of penetration of marker horizons in the different wells, the data is not decisive enough to be able to conclude with confidence about whether there is a tectonic structure present or if it was the case of the lava having been eroded or thinned out.

Keeping this in mind, other features were tested to verify if there was any positive relation between the permeability and the tectonic structures inferred in the area of Cachaços-Lombadas, such as plotting the location of the major permeable zones encountered in each well against the tectonic lineaments inferred in the area.

As referred to above, the entry into reservoir conditions is marked by the transition into the basalt lava sequence. Here, most of the permeability seems to occur between -150 and -400 m m.s.l. It is noticeable that the location of the permeable zones identified in CL4-A, CL5, and CL6 coincides roughly with the alignment of an inferred fault, oriented NNW-SSE, as shown in Figure 12. The same is observed with CL7 which was drilled towards WNW, crossing a NNW trending fault at about -300 m m.s.l. The location of the major permeable zone at CL7 is at -130 m m.s.l., and therefore higher than the expected

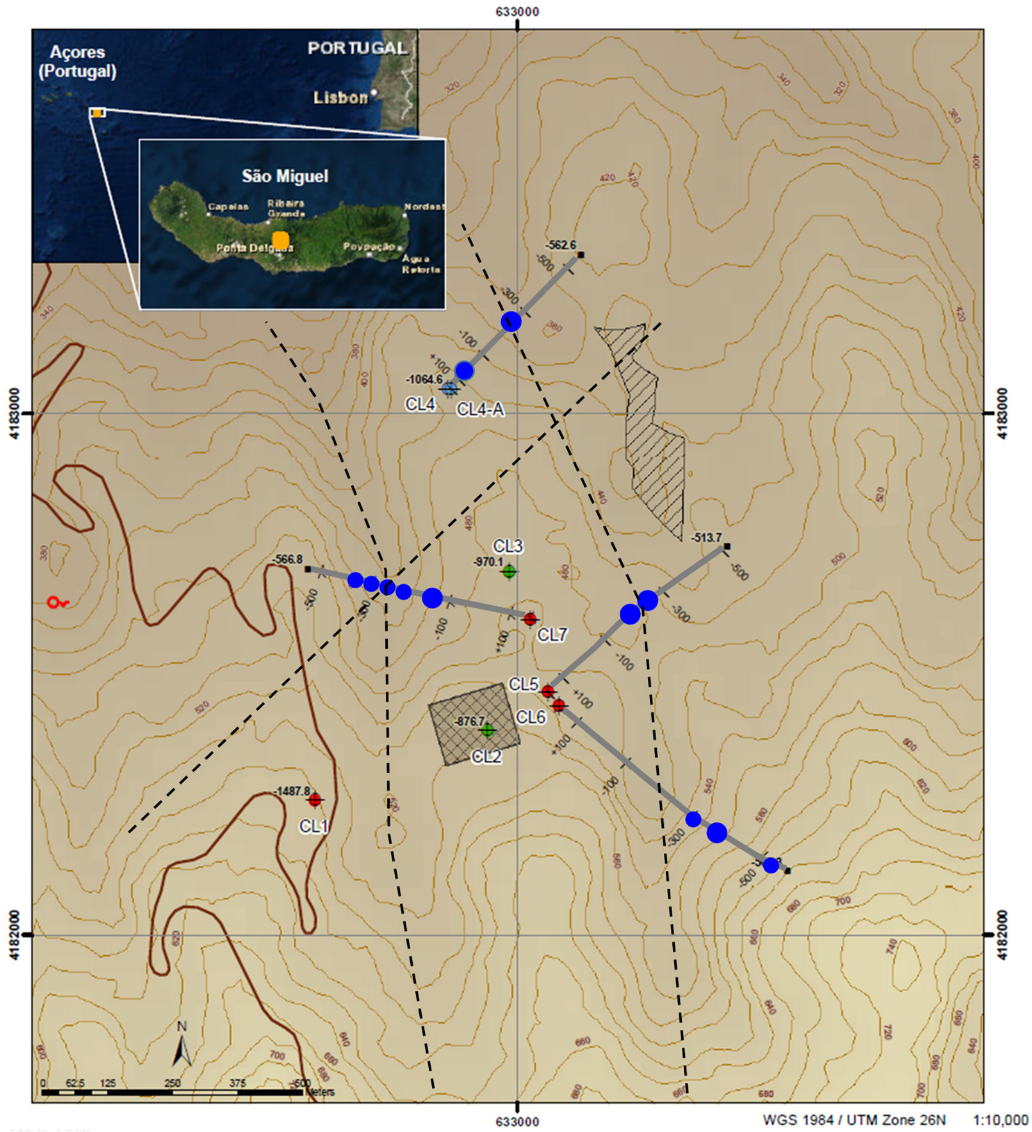

FIGURE 12: Map of Cachaços-Lombadas sector, Ribeira Grande Geothermal Field (adapted from GeothermEx, 2014). The map shows the location and well-path of the geothermal wells, including the location and size of the permeable zones (marked in blue circles) and the Ribeira Grande power plant, marked as a grey square. The dashed lines correspond to the inferred faults by Carvalho et al., 2006

intersection with the fault zone. However, it is noticeable that several minor feed zones were identified in CL7 at about -280 to -340 m m.s.l. and these are possibly related to the fault zone.

Either way, if the inferred faults indeed extend from the surface to deeper levels (this is uncertain), at least down to -400 m m.s.l., the deviated wells must have intersected the fracture zone related to these faults at some point. In this respect, it is worth noticing that the most prolific wells in the area are, by this order, CL7 with a wellbore trending to WNW and CL5 with a wellbore trending to NE. Additionally, well testing at CL4-A also revealed that this well could be an adequate producer. Therefore, this suggests that deviated wells that have intersected the NNW structural trend tend to be more productive.

5. FORMATION TEMPERATURE

The formation temperatures, based on stabilized profiles taken prior to injection or flowing, were gathered and plotted as a function of the elevation for all the Cachaços-Lombadas wells. In general, the temperature profiles show a similar pattern. As shown in Figure 13, the temperature gradient is relatively high to about -100 m m.s.l. and from there on the profiles are relatively isothermal, reaching maximum temperatures of about 230-240°C. A slight temperature reversal is observed in most of the wells (CL1, CL2, CL3, CL4, CL4-A). This strongly indicates that the main upflow zone of the geothermal system is not located in the central parts of the project development, in the area of Cachaços-Lombadas. Additionally, as shown in the Appendix III, most of the wells have a two-phase or steam zone on the top of the reservoir, with the only exception being CL6, located further to the south which only exhibits the liquid phase.

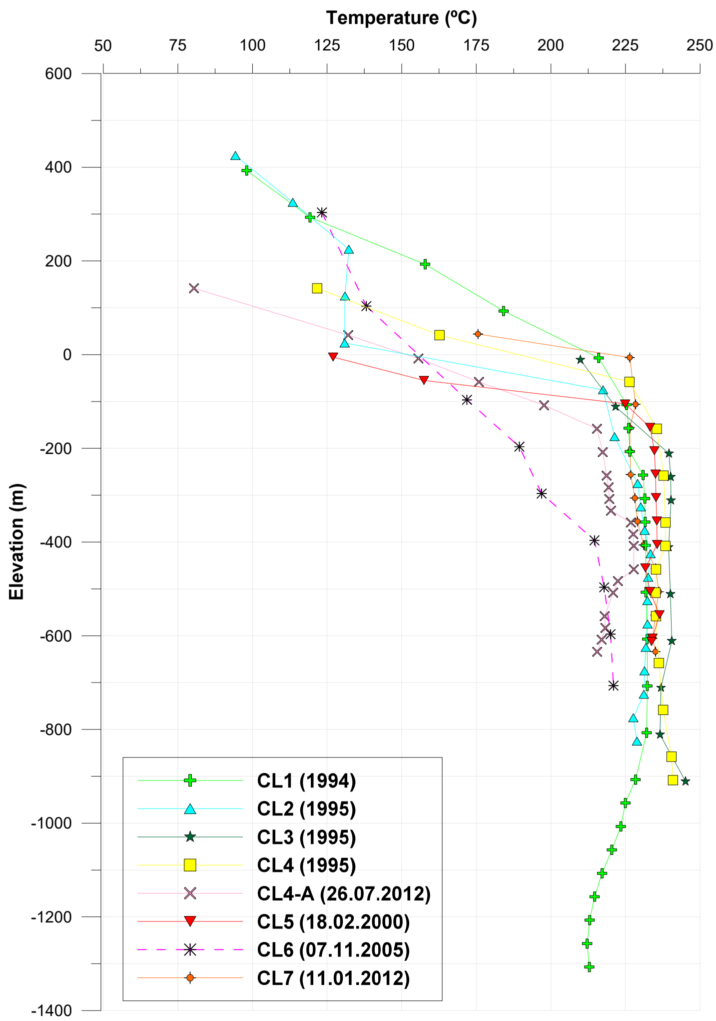

FIGURE 13: Formation temperature profiles of the Cachaços-Lombadas wells

The distribution of the formation temperature at four different elevations (0 m, -300 m, -600 m and -900 m m.s.l.) was inferred from temperature profiles. Figure 14 shows the temperatures contour maps drawn at 0, -300, -600 and -900 m m.s.l. The main findings from the analysis of the temperature distribution are in line with the conclusions from Ponte et al. (2010) and they can be summarized as follows:

- The temperature distribution at 0 m, still above the reservoir, shows that higher temperatures are found in the central and southwestern part of the Cachaços-Lombadas project development, with temperatures higher than 210°C being found in the wells CL7, CL2, and CL1;

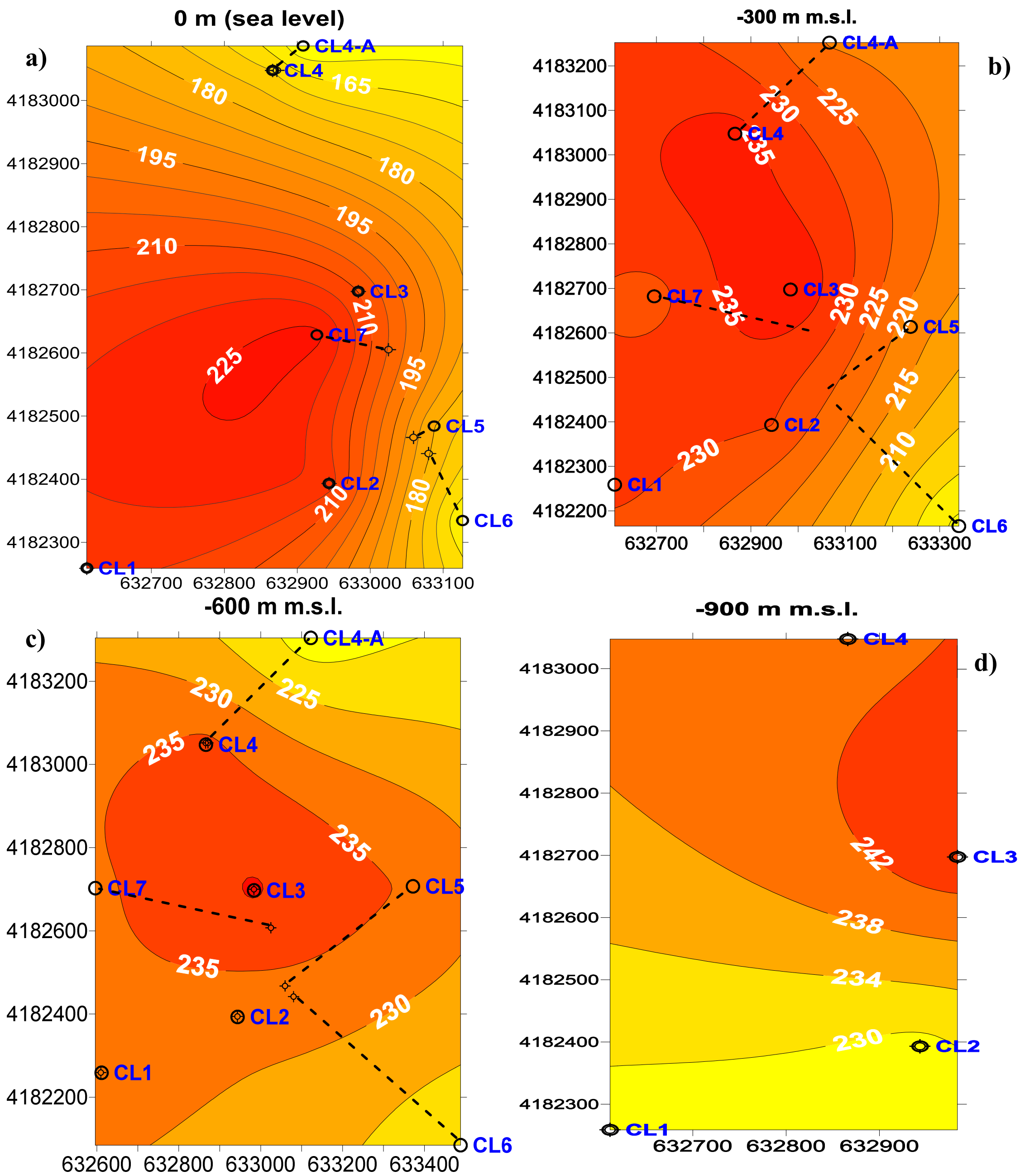

FIGURE 14: Temperature distribution in the area of Cachaços-Lombadas at 0 m (a), -300 m m.s.l. (b), -600 m m.s.l. (c) and -900 m m.s.l. (d). The dashed lines show the well-path of the deviated wells

- At -300 and -600 m m.s.l. the temperature maps are near isothermal with the temperatures ranging from 230-235°C in most of the area and with the highest temperatures being measured at CL3 (240°C). This depth interval corresponds to the core of the geothermal reservoir.
- With increasing depth, the temperatures continue to increase towards north and northeast whereas in the southern part of the area the temperatures tend to decrease. In fact, reservoir temperatures decrease towards CL6 which is somewhat cooler than the other wells, with maximum reservoir temperature that does not exceed 222°C.
- The data are insufficient to precisely locate the upflow zone because the majority of the wells were drilled only to about -600 to -700 m m.s.l. Nevertheless, as it deepens, the temperature distribution suggests that the main upflow zone may occur at some undetermined location to the east or northeast of wells CL3 and CL7.

6. HYDROTHERMAL ALTERATION

Reaction of geothermal fluids with the host rocks in the Cachaços-Lombadas sector has resulted in a progressive hydrothermal alteration sequence with increasing depth. However, it is important to note that the type and intensity of the alteration in the area also varies depending on the rock type present, showing locally strong or weakly altered zones. Commonly, the pyroclastics are less dense and tend to be more easily altered, whereas the dense lava flows tend to be fresher looking, although strong veining zones can occur within the lavas.

The alteration minerals assemblages found in Cachaços-Lombadas are typical for the wells in the Ribeira Grande field and are similar to what is found in other geothermal fields around the world in similar environments. Secondary minerals that were identified by binocular analysis included clay minerals, iron oxides (mostly hematite), silica minerals (such as opal, chalcedony and quartz), calcite, pyrite and zeolites.

Detailed petrographic analysis was limited to samples from well CL6. In this respect, the present study uses the findings from the investigation performed by the Foundation of the Science Faculty at the University of Lisbon which was contracted in 2005 by EDA RENOVÁVEIS, at that time denominated as SOGEO, to analyse thin sections from twenty drill cutting samples. The results from 2005 confirmed the occurrence of the minerals described above and allowed to identify others that are typical from high enthalpy hydrothermal systems such as secondary albite, epidote, prehnite and different zeolite types, including low and high temperature ones.

Additionally, X-ray diffractometric (XRD) analysis performed on selected samples from all the wells allowed the identification of the type of secondary clay minerals present. A total of twenty-seven samples were analysed using Bruker AXS D8 Focus Diffractometer at ISOR (Icelandic GeoSurvey) with the objective of determining the alteration zones within the Cachaços-Lombadas area. The present study also incorporates results from XRD investigations executed in 2005 by the Foundation of the Science Faculty at the University of Lisbon and in these are included seven samples from CL6 and three samples from CL5. The complete results from the XRD analysis are shown in the Appendix IV.

The abundance and the first appearance of the alteration minerals as function of depth is shown in the geological logs in Appendix II. Based on the occurrence, distribution and relative abundance of the secondary minerals it was possible to delineate the alteration zone diagrams from wells CL4-A, CL5, CL6, and CL7, described below in sections 6.1 to 6.4. The diagrams reflect the range of hydrothermal minerals that were found in each well and in general these vary from low temperature zeolites to high temperature minerals like chlorite, prehnite, epidote, and albite.

6.1 CL4-A

In CL4-A, based on the results from the binocular analysis to the drill cuttings and the XRD analysis to 9 samples, three alteration zones were inferred. As shown in Figure 15, these are unaltered to weakly altered zone, smectite zone and chlorite zone, which are summarized below:

0-185 m: *Unaltered to weakly altered zone*. This zone corresponds mainly to the thick sequence of trachyte lavas intersected in the well from 24 to 182 m. These lavas are relatively fresh and unaltered, exhibiting only weak clay alteration and locally oxide staining in the sanidine phenocrysts.

185-512 m: *Smectite zone*. The top of the zone is marked by the peaks in the clay and iron oxides alteration, identified at the bottom of the trachyte lava. In this zone, smectite is the dominant clay type, locally found associated with traces of illite. Calcite first appears at 196 m, becoming common thereafter. In this respect, two peaks in the abundance of calcite were identified, a first one at 320-340 m and a second one at 480-500 m. Secondary silica first appears at 230 m with opal and chalcedony

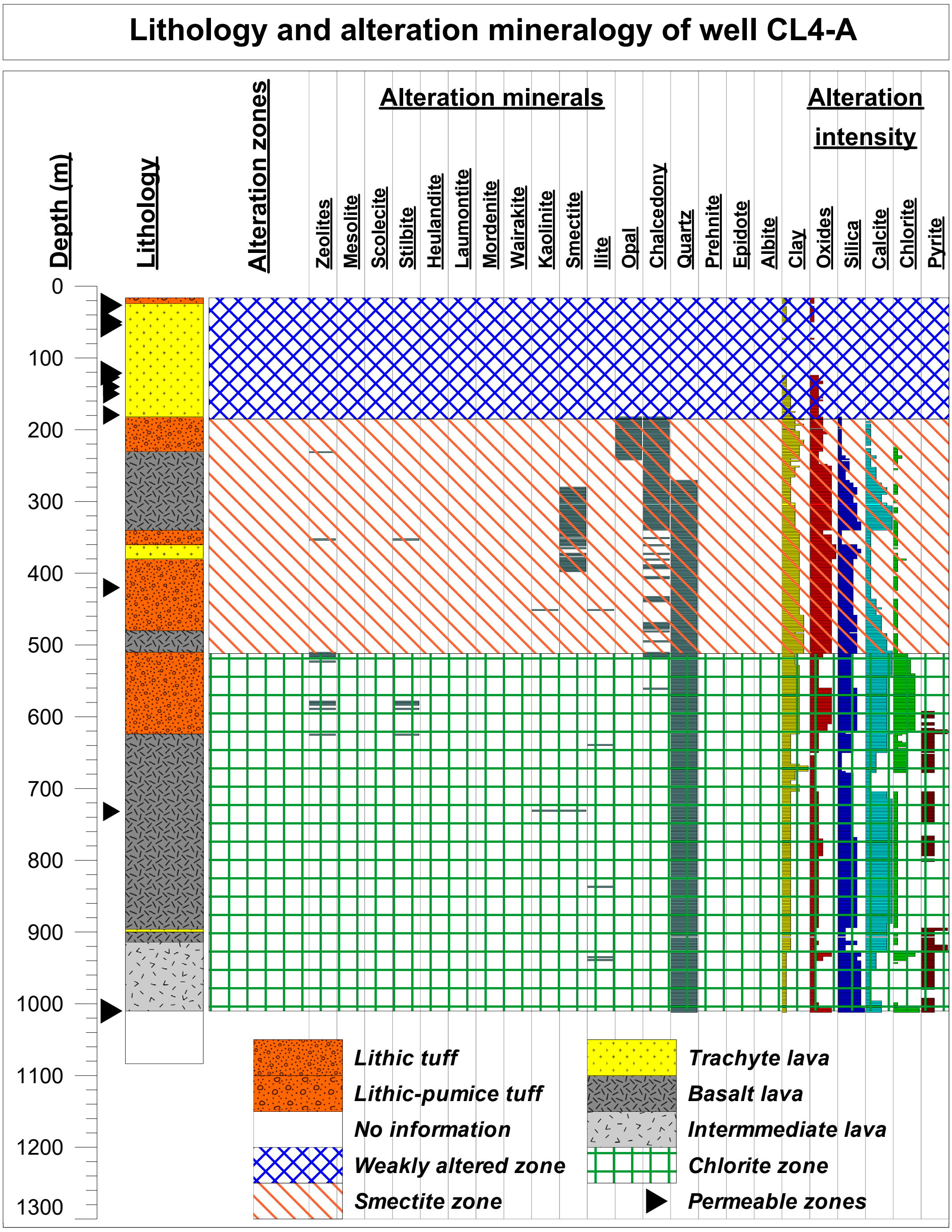

FIGURE 15: Alteration zones interpreted in CL4-A

amygdales in vesicular basalt lava. First appearance of microcrystalline quartz is at 270 m in veins and veinlets, where it is associated with calcite and possibly very fine chlorite. From there, quartz becomes common and persists down to the bottom of the zone. Chalcedony and possibly zeolite amygdales are also found intermittently at the bottom of the zone, but the positive identification of the latter could only be possible by a detailed petrographic analysis.

512-1010 m: *Chlorite zone*. The upper part of this zone is marked by a peak of open-space fillings found at 510-520 m with the mineral assemblage mainly composed of different associations of chlorite, quartz and calcite. Pyrite appears at 564 m and this is relatively deep compared to the other existing wells. From there, pyrite persists to the depth of the last sample recovery but it is seen intermittently and in minor quantities. In this zone, the ash matrix of the pyroclastics is often altered to clay with the chlorite and minor traces of illite forming the main clay types. The ash matrix is locally indurated by silicification, likely as result of deposition of chalcedony or microcrystalline quartz. With depth, veins, veinlets and amygdales of the assemblage calcite + quartz + chlorite continue to be generally abundant, mainly occurring within the lavas intersected in this interval. It is important to note that chlorite abundance decreases with depth but it peaks again just before a major permeable zone was found at 1010 m.

6.2 CL5

In CL5 (Figure 16), based on the data from the binocular analysis complemented by XRD difractometry analysis to 8 samples and petrographic analysis to three samples (620, 670 and 703 m), three alteration

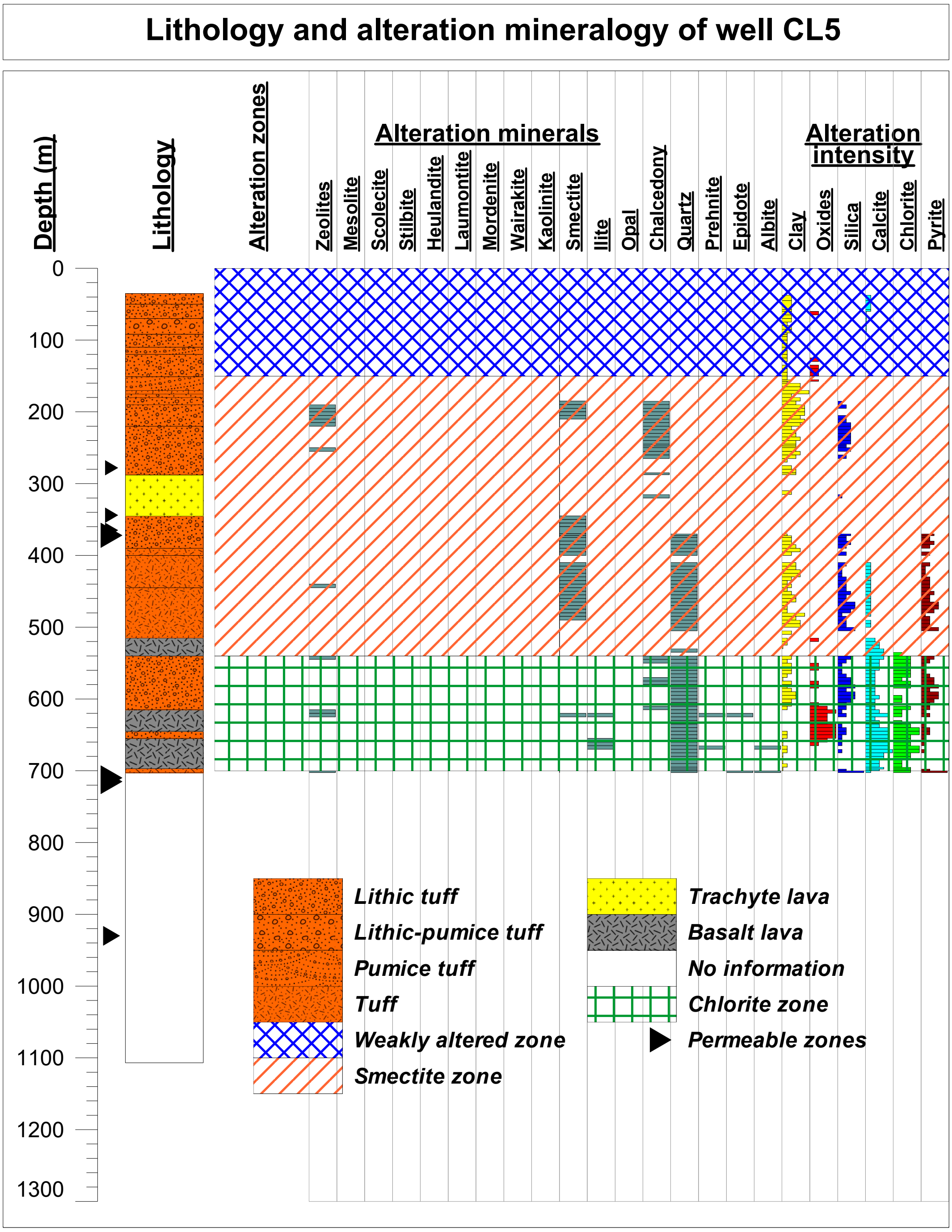

FIGURE 16: Alteration zones interpreted in CL5

zones were interpreted. These are weakly altered zone, smectite zone and chlorite zone, and they are summarized below:

0-345 m: *Weakly altered to unaltered zone*. The alteration within the first 150 m consists mainly of the conversion of the glassy components (ash and pumice) of the pyroclastic rocks to clay minerals. Iron oxides are locally abundant. Small amounts of calcite and opal appear at 50 m and are present to the bottom of the zone in small quantities.

150-540 m: *Smectite zone*. A trend induration of the matrix of the pyroclastic units begins at 150-200 m and it becomes more intense at about 250 m, as a result of the deposition of silica (probably opal). Silica persists with depth but it stops in the trachyte lava intersected at 288-345 m which is relatively fresh and unaltered. Underlying the trachyte lava, the pyroclastic rocks are variable altered. This zone is characterized by the abundance of smectite clay and silica minerals which are more crystalline when compared to the upper zone, suggesting that chalcedony and microcrystalline quartz are now the dominant silica mineral phases, replacing opal which dominated above. At this respect, the first appearance of quartz is logged at 370 m. Veining appears to be absent, with the only exception being a scoria unit at 445-555 m, exhibiting silica veins.

540-700 m: *Chlorite zone*. Alteration peaks at 540 m with the chlorite and calcite becoming the most abundant secondary minerals, occurring as replacements of most of the rock components but also in veins and other open-space fillings. Quartz and pyrite complete the secondary mineral assemblage. Hematite is also locally important, particularly in the basalt lava found at 615-645 m, being found in many places where it has been clearly recrystallized and sometimes mobilized as a vein mineral. Hematite and pyrite often coexist, with pyrite replacing hematite in some places. In this zone, veining appears to increase in intensity with depth, reflecting increasingly intense hydrothermal activity. The vein minerals include quartz, calcite, chlorite, pyrite and hematite, found in various different assemblages. The detailed petrographic analyses from 2005 revealed that prehnite is found locally at 620 m, being associated with calcite. The same is with epidote which first appears at 620 m. The bottom of the zone is marked by the appearance of secondary albite which is often found with epidote + calcite + quartz + chlorite.

6.3 CL6

In CL6, three alteration zones were interpreted as shown in Figure 17. These are a weakly altered zone, a smectite zone and a chlorite zone. They are summarized below:

0-196 m: *Weakly altered to unaltered zone*. At shallower depths and down to 196 m the alteration consists predominantly of the conversion of ash and pumice into clay minerals. Iron oxides are locally present in minor amounts but most of these are likely a product of superficial weathering prior to burial. Opal is locally present.

196-590 m: *Smectite zone*. Below 196 m smectite is the predominant clay mineral, locally associated with illite aggregates. The zeolites found in the top of this zone are low temperature types such as mesolite, scolecite, stilbite and heulandite/laumontite, commonly appearing in amygdales. Other open space fillings found at the top of this zone are mostly chalcedony and microcrystalline quartz, but calcite and very fine chlorite are also present with the latter being identified in the petrography analysis. Overall the alteration is low-grade but it peaks near 270 m. There is a zone of stronger mineralization within the trachyte lava intersected at this depth with clusters of pyrite, calcite and microcrystalline quartz. The same formation was intersected by the nearest well CL5 but this mineralized zone was not found in CL5, suggesting that the mineralization may be associated with a specific fracture zone passing through the lava in the area of CL6. Below 350 m the microcrystalline quartz becomes more abundant comparatively with chalcedony and the more abundant zeolites are heulandite and laumontite. Below 500 m veining becomes common, with mineral assemblages of quartz, calcite, fine chlorite along with silicification of the rock, namely the interstitial spaces of the rock fragments.

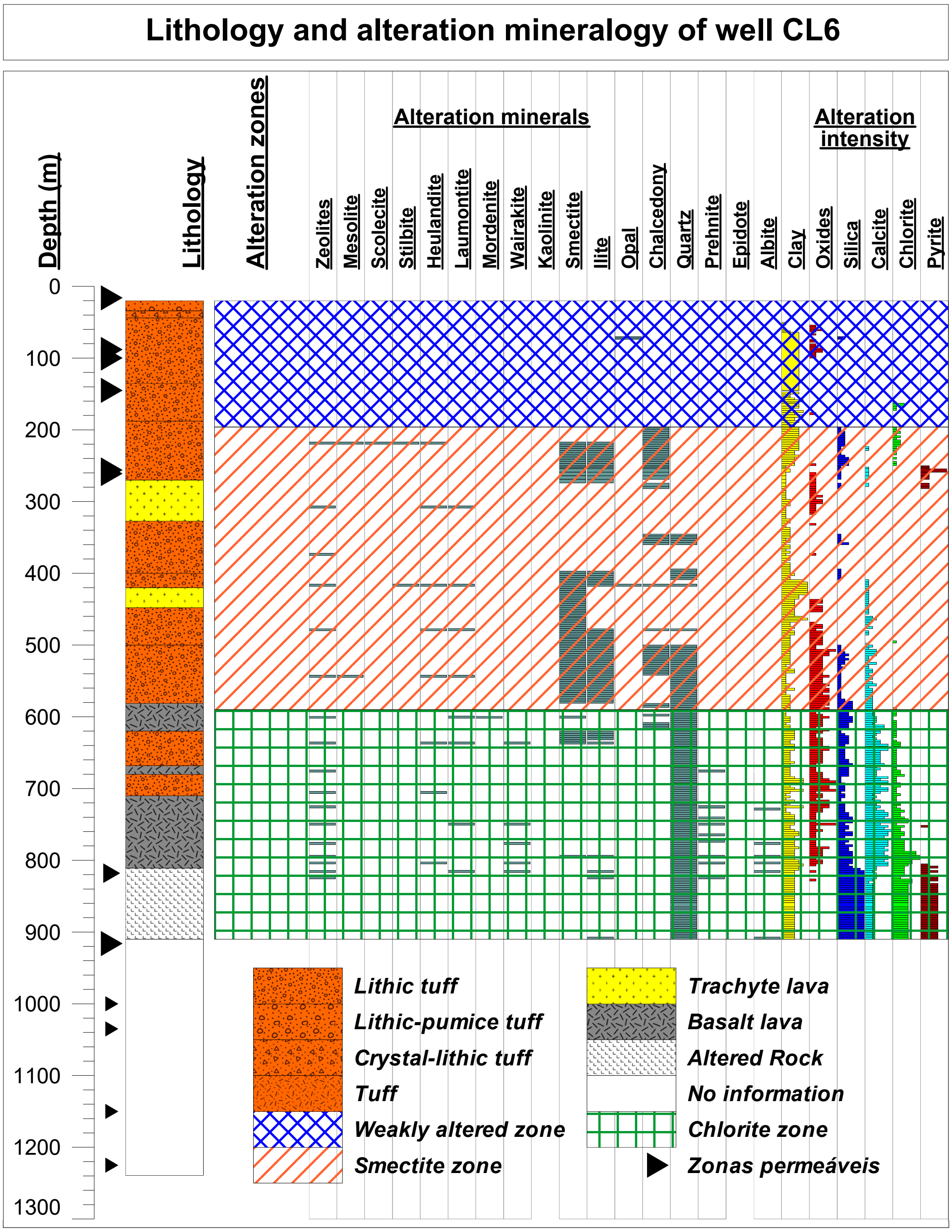

FIGURE 17: Alteration zones interpreted in CL6

590-775 m: *Chlorite zone*. Chlorite is rare above 590 m but it becomes abundant thereafter, marking the top of this zone. The alteration assemblage of quartz + calcite + chlorite is common throughout this zone, appearing as open-space fillings, suggesting that the basalt lava and pyroclastics found at these depths are characterized by a large net of veins and veinlets filled with secondary minerals. Here, it is important to note that the abundance of calcite and chlorite increases with depth, whereas the abundance of the other secondary minerals appear to vary within more a less constant ranges. At the top of the zone the predominant zeolite type is laumontite, but heulandite and mordenite are also found in minor amounts. Wairakite appears at 635 m, suggesting alteration temperatures of up to 200°C. Detailed petrography from 2005 identified also the presence of high temperature minerals. Epidote was identified at 674 m, becoming common thereafter, associated with quartz, calcite, chlorite and prehnite. Secondary albite was identified at 775 m, locally associated with epidote. The mineral assemblages found at the bottom of the zone consist mainly of epidote + albite + chlorite + prehnite + calcite + quartz, indicating alteration temperatures in the range of 230-250°C.

6.4 CL7

In general, the alteration found in CL7 (Figure 18) is similar to the other wells in Cachaços-Lombadas area but the occurrence of a strong alteration zone at about 125-200 m is unusual. This zone is characterized by the abundance of white to light grey clay (mostly smectite and kaolinite) and disseminated pyrite (present in clusters and as well-developed cubic crystals with size up to 2 mm). This type of mineralization is typical of acidic environments, so this zone could be the product of a now

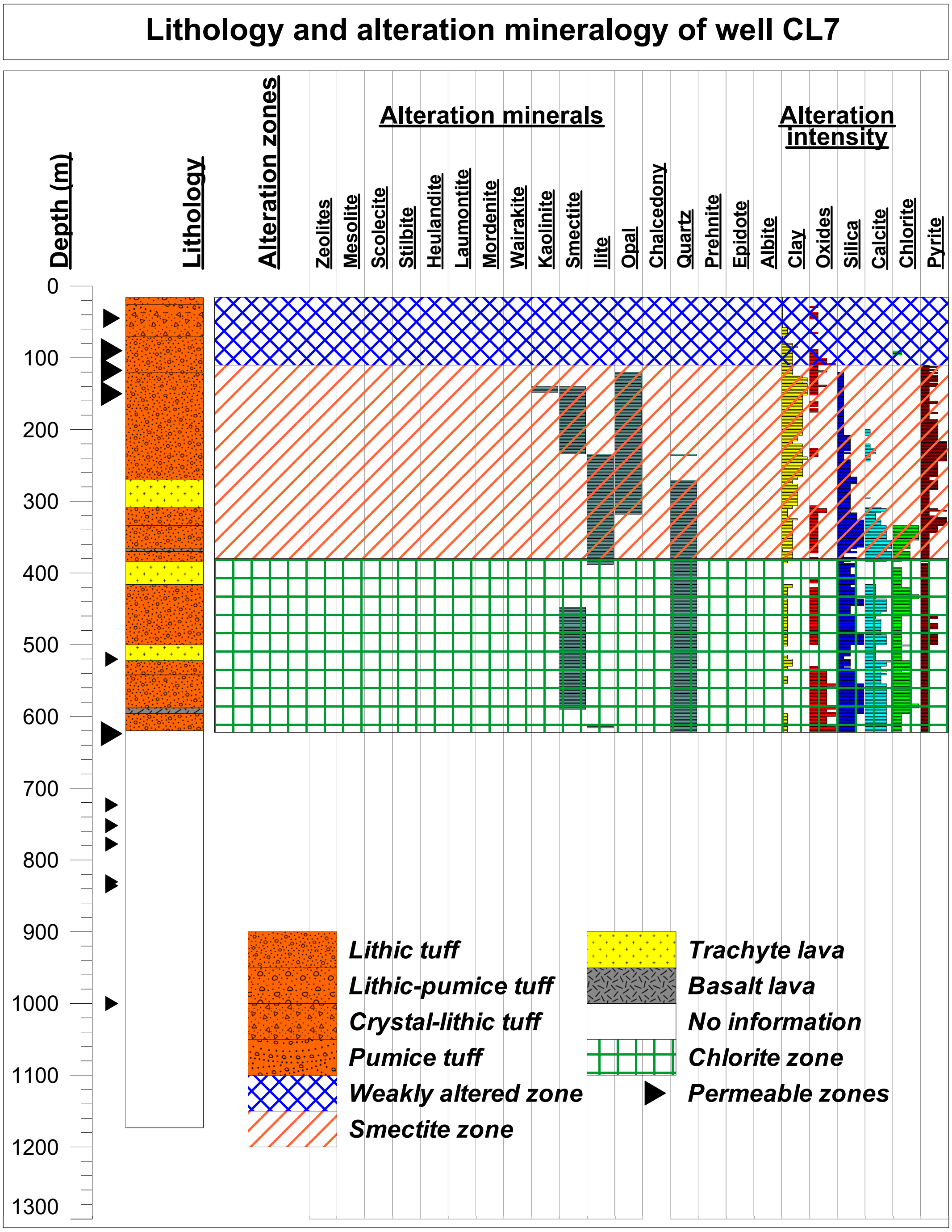

FIGURE 18: Alteration zones interpreted in CL7

extinct steam heated aquifer. No similar style of alteration was found in similar intervals in the wells CL4-A, CL5, or CL6.

0-110 m: *Unaltered to weakly altered zone*. The alteration consists mainly of the conversion of the glassy components (ash and pumice) of the pyroclastic rocks to clay minerals. Iron oxides are locally abundant but these may be a product of superficial weathering prior to burial.

110-380 m: *Smectite zone*. From 110 m the ash matrix of the pyroclastic rocks becomes indurated as a result of deposition of silica (likely as opal). Pyrite appears at 110 m and it is continuously encountered throughout the remainder of the well. The appearances of pyrite and quartz (found at 234 m) are relatively shallow compared to the neighbouring wells. In the bottom part of the trachyte lava occurring at 270-300 m, the formation is strongly altered to clay (mainly illite) and is overall mineralized with clusters of pyrite, calcite and probably microcrystalline quartz. From 360-384 m some well-developed hexagonal quartz crystals up to 1 cm in size were found. This is rather unusual as crystals of this size were not found in any of the other Cachaços-Lombadas wells.

380-622 m: *Chlorite zone*. The top of this zone is clearly marked by a peak in the chlorite alteration with the mineral assemblage being composed by clays (chlorite is dominant while illite appears in small trace amounts), silica, chlorite, pyrite, calcite and iron oxides. In the top part of this zone, a second sequence of trachyte lavas are found at 384-416 m and alteration appears to be more intense near the top, mostly corresponding to veining. Below 422 m, the pyroclastic units are moderately altered and contain abundant pyrite, including some well-formed cubic crystals. With depth, the formations continue to show increasing hydrothermal alteration and it becomes difficult to distinguish the original rock type. Overall, the rock formations are moderately altered to clay. Chlorite is the dominant clay type but smectite is consistently present as well, whereas illite was found only in minor traces below 614 m. Below 520 m there is a notable peak in open-space fillings abundance with different mineral assemblages of chlorite + silica + hematite + calcite + pyrite.

7. ALTERATION ZONING

The present study reveals two zones of hydrothermal alteration beneath a shallow zone of relatively unaltered rocks. A summary of these zones is presented below:

- *Weakly to unaltered zone.* Extending from the surface to about 150-200 m depth, the formations in this zone are relatively fresh and unaltered, with little or no signature of alteration or development of any secondary minerals. Pyroclastic rocks are the predominant lithological unit and the alteration consists of the conversion of ash and pumice into weak clay and locally minor oxide staining of the feldspars in the lithic fragments;
- *Smectite zone (<200-220°C)*. The hydrothermal alteration generally starts at 150-200 m and this marks the beginning of the smectite zone which extends down to 510-590 m. In this zone, smectite is the predominant clay type, mostly resultant from the alteration of the ash matrix of the pyroclastic rock units. It is important to note that the lava flows found in this zone are denser than the pyroclastics so the clay alteration is generally less intense in these, even though veining is often seen in the lavas. The smectite zone is also characterized by the increasing silicification of the rock formations with depth which is accompanied by the progressive deposition of the silica mineral phases, namely opal, followed by chalcedony and quartz. Overall, the alteration in this zone is generally low grade and the mineral assemblage at the bottom of this zone indicates alteration temperatures that do not exceed 200-220°C.
- *Chlorite zone* (>230°C). The transition to the chlorite zone is marked by the peak in the chlorite abundance, commonly found in mineral assemblages along with calcite and quartz which are found in open-space fillings. This indicates that the formations in this depth range (predominantly basalt lavas) are characterized by dense net of veins and veinlets filled with secondary minerals. It is important to note that, at the top of this zone, chlorite and smectite

were seen to coexist in some places (see Appendix V), indicating that the upper part of the chlorite zone might correspond to a transition zone. Furthermore, with increasing depth, smectite disappears and chlorite becomes the dominant clay mineral. The Chlorite zone is also marked by the appearance of high temperature minerals such as prehnite, epidote and albite which were identified in CL5 and CL6 below 650 m. This corresponds to the reservoir interval where the mineral assemblage is frequently completed with chlorite and indicates alteration temperatures above 240-250°C.

The alteration zones from the four wells were plotted together with the lithology and temperature isograds from key index minerals in order to understand the general distribution of the alteration temperatures in the Cachaços-Lombadas area. As shown in Figure 19, the alteration zones have a consistent distribution with depth and show a relatively good correlation from well to well. The zoning pattern indicates that smectite and chlorite zones are shallower in CL7 when compared to the other wells. This becomes more evident for the chlorite zone which was found at 100 m m.s.l in CL7, whereas in CL4-A, CL5 and CL6 it was found at -80 to -100 m m.s.l. Therefore, the zoning pattern indicates that higher alteration temperatures were found shallower at the location of CL7, suggesting that CL7 is probably closer to the heat source than the other wells. It is important to note that this evidence is consistent with the formation temperature distribution within the area as discussed in section 5.

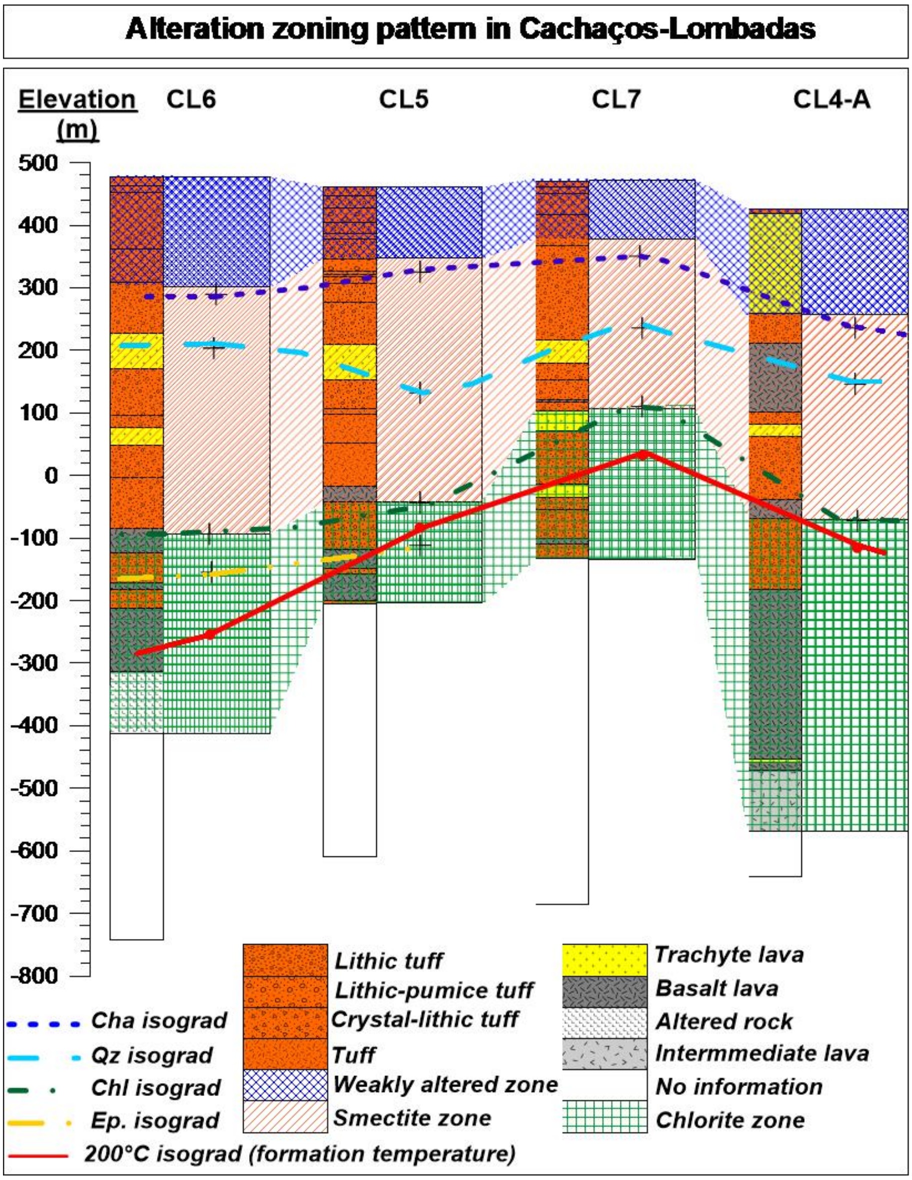

FIGURE 19: Alteration zoning diagram of Cachaços-Lombadas area

Additionally, by comparing the alteration temperature isograds from key index minerals against the isograd of 200°C (formation temperature) it is possible to observed that the chlorite isograd, which indicates past temperatures of at least 230°C, is found above the 200°C isograd in all the wells. This evidence indicates that higher temperatures were present shallower at some point in the past.

8. STUDY OF FLUID INCLUSIONS

The study of fluid inclusions can be used for geothermometry and it is most commonly applied to study the evolution of geothermal systems as a complement to the information provided by the alteration mineralogy. Additionally, fluid inclusions are an important tool to determine the chemical compositions of the geothermal fluid in the past.

8.1 Heating studies

In the attempt to determine the thermal history of the geothermal system in the area of Cachaços-Lombadas a total of nine samples from CL4-A, CL5, and CL7 were used in heating studies for determination of the homogenization temperatures (Ht). This investigation complemented by the identification of the first appearance and abundance of key index secondary minerals (as described in sections 6 and 7 above) provided valuable data on the historical deep temperatures and contributed to the determination of the alteration temperature curves. During the present study, it was noticeable that quartz samples from the Cachaços-Lombadas wells contain different types and numerous generations of fluid and gas inclusions and special care must be taken in the assignment of a given inclusion or group of inclusion to a particular paragenetic stage.

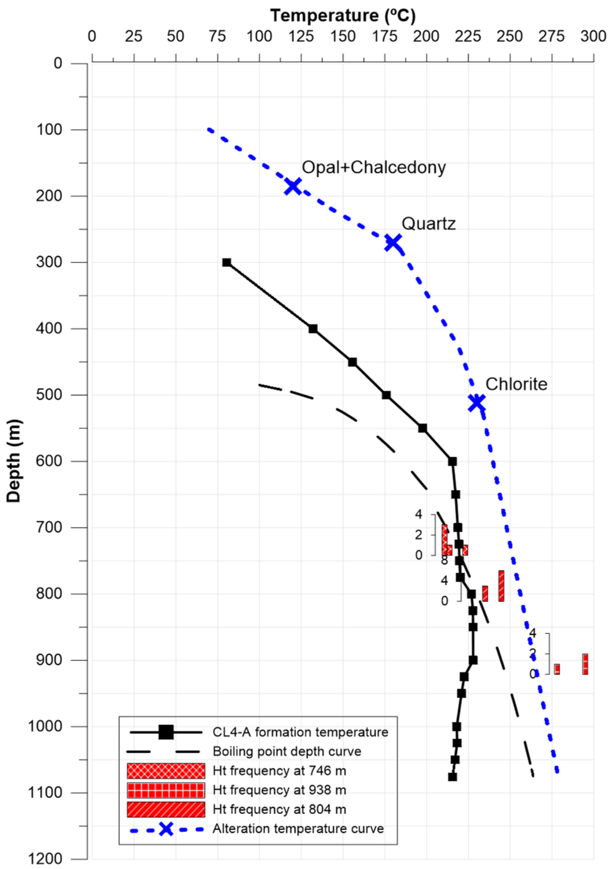

FIGURE 20: Homogenization temperature range from fluid inclusions of CL4-A along with the formation and alteration temperature curves

8.1.1 Samples from CL4-A

CL4-A is the well that has the deepest geological record available in the area of Cachaços-Lombadas because total losses of circulation were only encountered at 1010 m what is significantly deeper in comparison to the other Cachaços-Lombadas wells. This allowed for sampling of an important sequence of the reservoir interval. During the binocular analysis of the rock samples, quartz crystals from veins found in samples from 746, 804, and 938 m were selected for the study of fluid inclusions. This selection was based on the crystal abundance at those intervals (samples 804 and 938 m) as well as the proximity or direct occurrence at inferred permeable zones of the well (sample from 746 m).

As shown in Figure 20, the results show increasing Ht with depth with temperatures ranging between 211-223°C at 746 m to 278-295°C at 938 m. Noticeably, homogenization temperatures at 746 m have a good fit with the formation temperature but with increasing depth there is a growing shift between the formation and the homogenization temperatures, suggesting that the geothermal system at the location of CL4-A was at some point in the past significantly hotter that it is today reaching temperatures close to 300°C.

8.1.2 Samples from CL5

The entry into reservoir conditions is well marked at CL5 by the abundance of veining in the interval from about 540 to 660 m depth. Thus, quartz crystals from samples at 550, 610 and 650 m were selected for the study of fluid inclusions (Figures 21 and 22).

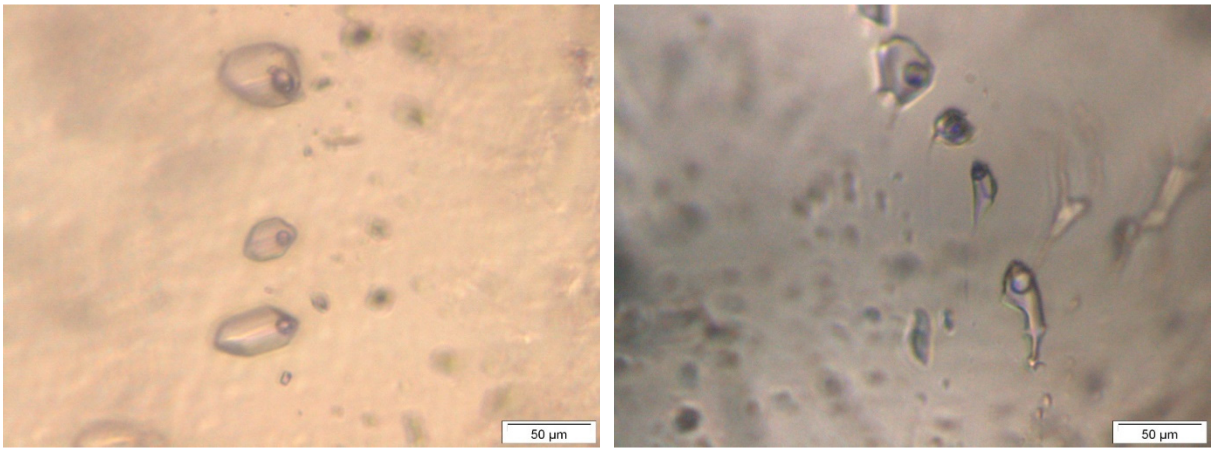

FIGURES 21 and 22: Fluid inclusions of quartz crystals from CL5. To the left inclusions from the 550 m sample are shown and to the right inclusions from the 610 m sample are shown

As shown in Figure 23, the homogenization temperatures in the CL5 range from 200 to 270°C with the lowest temperature being measured at 610 m. Nevertheless, considering the frequency of the Th measurements, the most common temperatures are ranging from 225 to 260°C. Additionally, there is an evident tendency for the homogenization temperatures to increase with depth and this is a similar pattern to what was seen in CL4-A but here the Th gradient is smaller than in CL4-A.

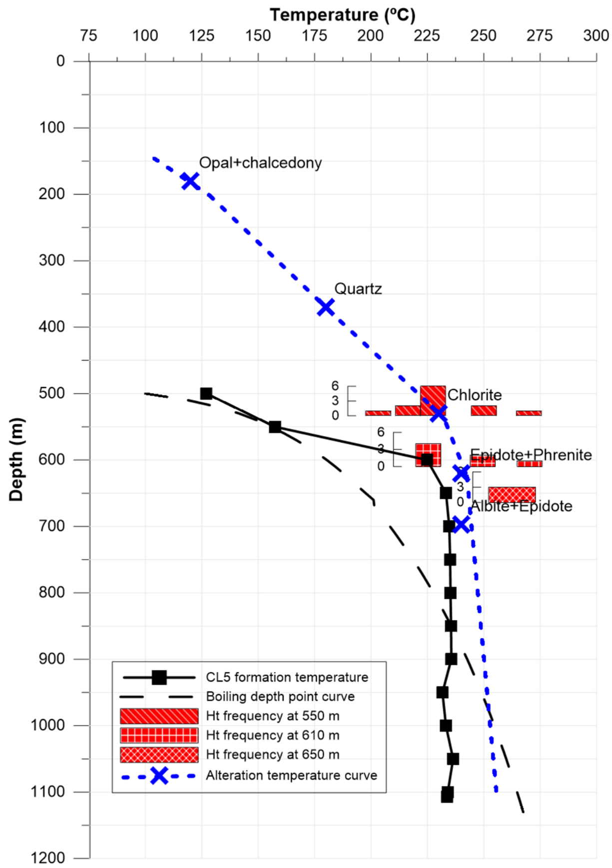

FIGURE 23: Homogenization temperature range from fluid inclusions of CL5 along with the formation and alteration temperature curves

Moreover, the homogenization temperatures are slightly higher than the formation temperatures, suggesting that at the location of CL5 temperatures within the geothermal system could have been slightly hotter at some point in the past than they are today, possibly ranging from 235-270°C. Moreover, based on the Th results, reservoir temperatures (above 225°C) were present in the past at 550 m what is slightly shallower than at present times. This observation suggests that the fluid level within the reservoir was at some point in the past at slightly shallower depths than today. This is consistent with the secondary mineralogy found at around 540 m depth where the rock formation starts to show abundant veining which becomes common and appears to increase in intensity with depth, reflecting an increase in the hydrothermal activity. Here, the vein mineral assemblages include calcite, quartz, chlorite, pyrite and hematite which can be found in different combinations. Thus, the common association of calcite and quartz, as well as the identification of deposition of different calcite generations with distinct grain size and optical properties (Foundation of the Science Faculty at the University of Lisbon, 2005), suggests that fluid levels within the geothermal system had been fluctuating in the past.

8.1.3 Samples from CL7

From well CL7 the selection of samples was limited to the initial 620 m because almost the entire reservoir interval was drilled without returns. CL7 shows strong silica alteration starting from 150-200 m depth onwards with initial deposition of opal. With depth, first chalcedony and then microcrystalline quartz replace opal as the silica phase. In the interval from 200 to 500 m two samples of well-developed hexagonal quartz were found at 234 and 464 m and these were selected for the study of fluid inclusions. It is noteworthy that the size of the quartz sample found at 464 m (1.3 cm) is not very common in the Ribeira Grande field but similar size quartz crystals were occasionally found in other wells (for example at 254 m in well RG4, drilled in the Caldeiras sector of the Ribeira Grande Geothermal Field).

The fluid inclusions found in the quartz sample at 234 m showed homogenization temperatures ranging from 243 to 272ºC what is significantly higher than the estimated formation temperatures at this depth. The absence of logging points above 500 m depth in the temperature profiles obtained from the well makes it difficult to be certain of the precise formation temperature at 234 m depth but it is unlikely to exceed 175ºC which is the formation temperature measured at 500 m depth. It is noticeable that at about 150-250 m depth the rock formation exhibits intense argillic alteration with abundant white clay. X-ray diffraction results indicate that smectite is the dominant clay type at this depth where it was found coexisting with kaolinite at the top of the interval and with illite below 200 m. This type of clay alteration is a characteristic of acidic environments, suggesting that this could be the result of a now extinct steam heated aquifer.

The size of the 464 m quartz crystal allowed it to be cut in four transversal sections which are each about 1 mm thick for detailed fluid inclusion studies. From these samples, one from the top and another from the bottom were selected and heated to determine the homogenization temperatures of the fluids trapped in them.

The quartz sections were analysed under the microscope and it was possible to observe that they contained different generations of fluid inclusions which can be summarized as three types: i) some well-formed growth zones outlined by groups of primary fluid inclusions (Figure 24) predominantly correspondent to gas inclusions; ii) a few groups of secondary inclusions found aligned along micro fractures and were mostly liquid (water) but gas inclusions were also found; iii) isolated primary fluid inclusions with no specific relation to any growth zone of the crystal or any specific microfractures; these are predominantly liquid inclusions.

The primary inclusions were formed during the growth of the quartz crystal. During crystallization the quartz was fractured and when these micro fractures healed they trapped small quantities of the surrounding liquid or gaseous fluids in the host crystal, forming secondary inclusions. Both primary and secondary fluid inclusions were heated to determine the homogenization temperatures in an attempt to understand the thermal evolution of the geothermal system during the crystal grow. The main findings are described below.

- At the bottom of the crystal, the primary inclusions (primary to the growth of the crystal), show Ht of 240 to 290°C;
- Primary inclusions at the top of the crystal show Th of 227 to 251°C, meaning that a cooling episode of the geothermal system has occurred during the period of time at which the crystal was growing;

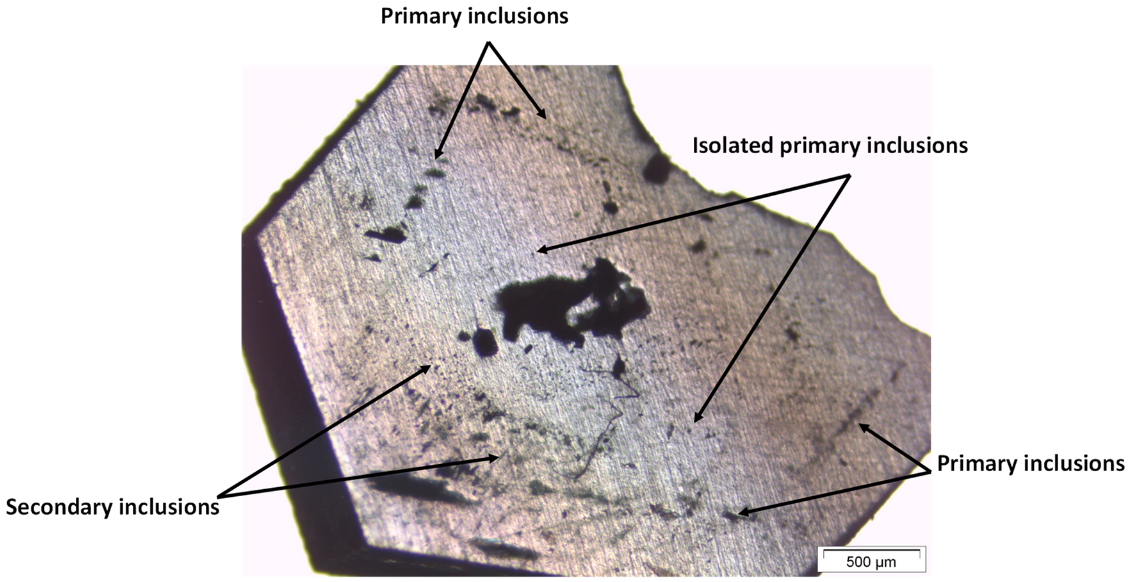

FIGURE 24: Top section of the 464 m quartz sample from well CL7

- Secondary inclusions found at the bottom (Figures 25 and 26) and at the top of the crystal show consistent Th in the range of 233-241°C. These are similar to the Th range shown by the primary inclusions found on the top of the crystal, indicating that the geothermal system was in equilibrium since the end of the crystal growth;
- When comparing the secondary fluid inclusions Th (233-241°C) with the formation temperatures seen today we observe that the range of temperatures given by the fluid inclusions is very similar to the present time reservoir temperatures found in the Ribeira Grande field, meaning that the geothermal system is in equilibrium since the end of the crystal growth;
- As shown in Figure 27, Th results seem to indicate that higher reservoir temperatures were present at shallower depths in the past what points at possible fluctuations in the fluid level within the reservoir;
- A significant number of gas inclusions were found in all the samples from CL7 (see Figure 28). This indicates that boiling was occurring when the gas was trapped during the quartz crystallization.

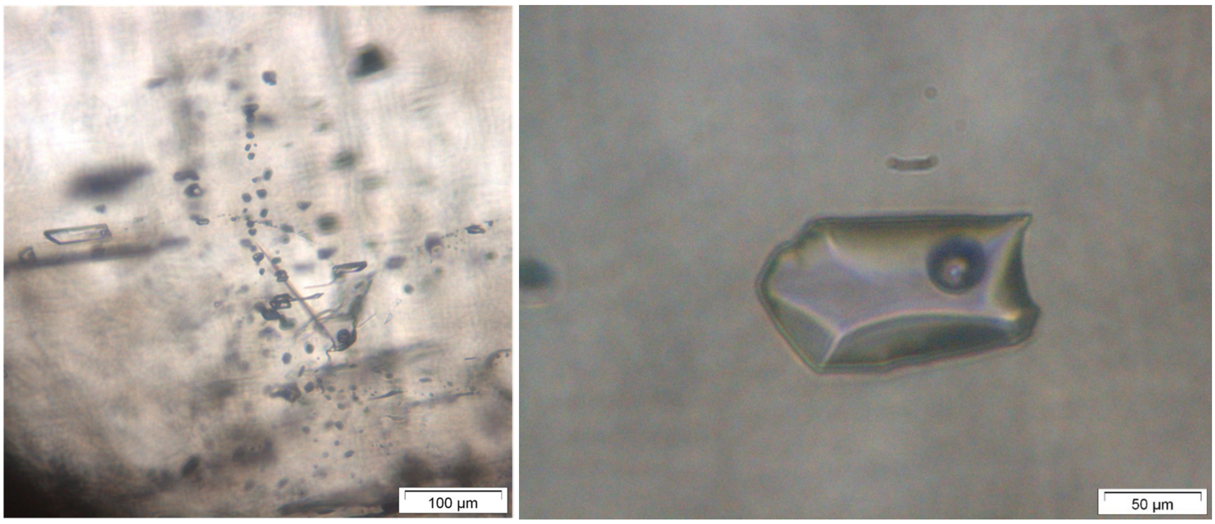

FIGURES 25 and 26: Secondary liquid inclusions with vapour bubble found at 464 m (bottom section of the quartz crystal)

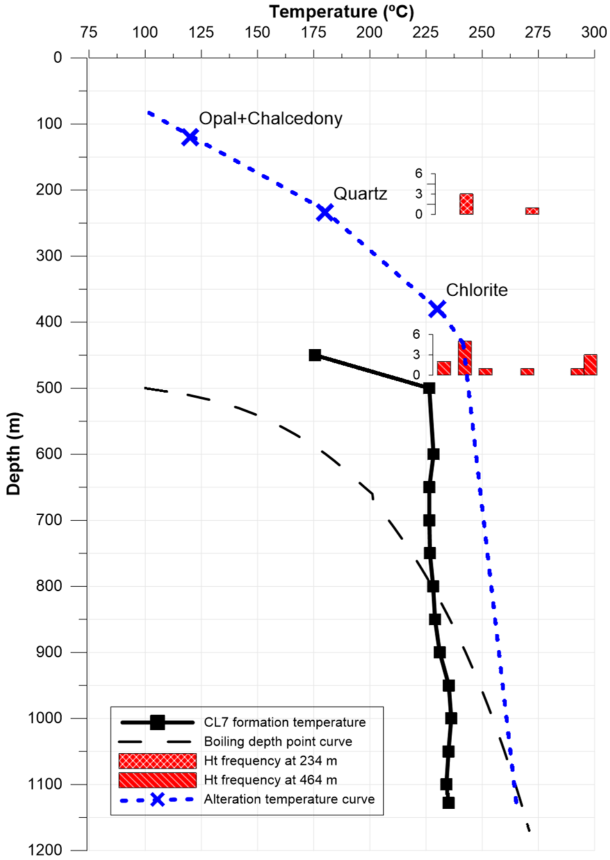

FIGURE 27: Homogenization temperature range from fluid inclusions of CL7 along with the formation and alteration temperature curves

8.2 Freezing studies

Two samples from CL7, namely the top and bottom sections of the 464 m quartz described in section 8.1.3, were frozen to determine the melting point temperatures (Tm) and investigating the composition of the liquids trapped in them (Figure 29). The melting temperatures were consistently -0.3ºC. According to Bodnar and Vityk, 1994, these melting temperatures correspond to 0.53wt% of sodium chloride salinity equivalent. These results indicate that the fluid within the geothermal system has consistently been composed of fresh water. This is in line with the present time chemical data from the geothermal fluid given by isotopic analysis which indicates that the recharge into the geothermal system is meteoric water (GeothermEx, 2008; Ponte et al., 2009; Pham et al., 2010; Ponte et al., 2010; Rangel, 2014).

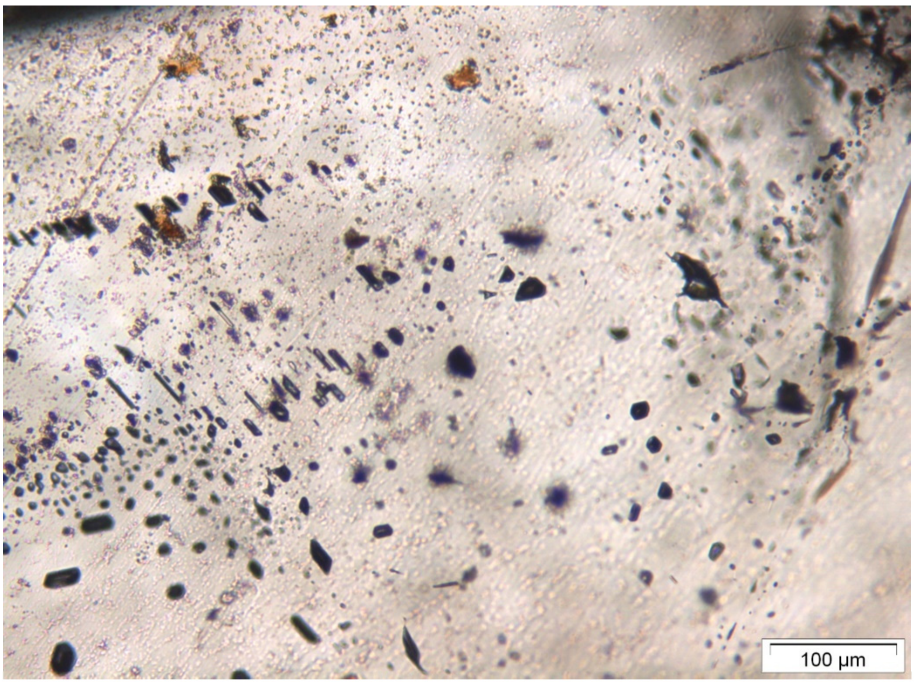

FIGURE 28: Groups of predominantly gas inclusions found in the 464 m sample (to section of the quartz crystal). The photo was taken at room temperature (22°C)

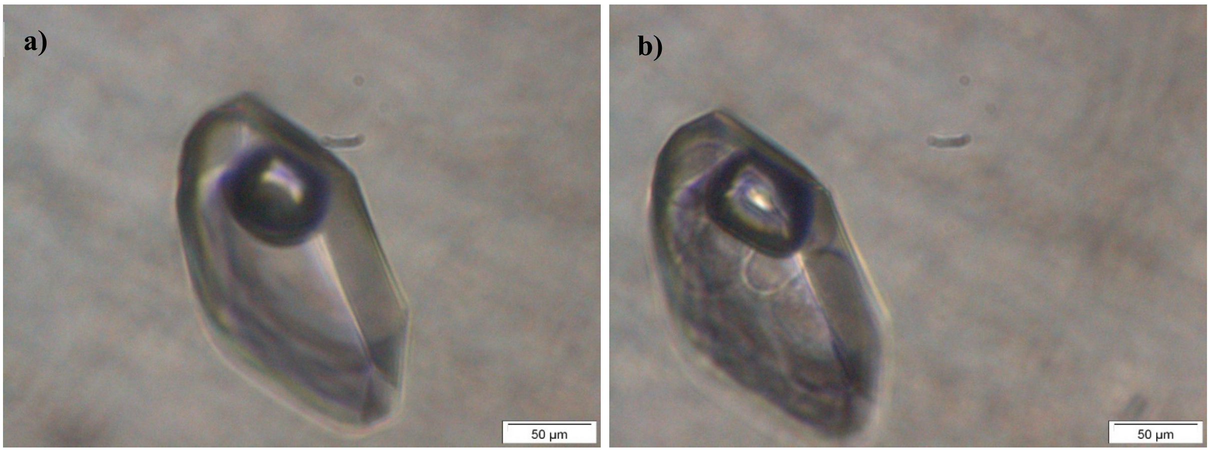

FIGURE 29: Fluid inclusion studied in the 464 m quartz of CL7. To the left the freezing stage is at -10.0°C and to the right the freezing stage is at -0.3°C where the ice melting becomes evident

9. COMPARISON BETWEEN THE ALTERATION TEMPERATURE AND FORMATION TEMPERATURES

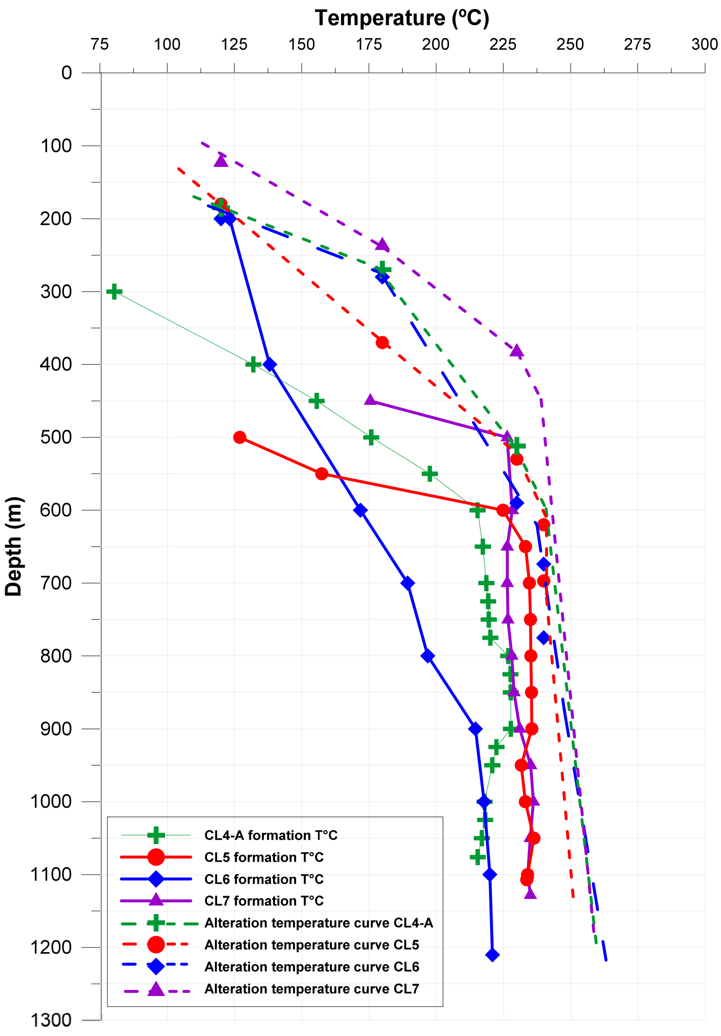

FIGURE 30: Formation and alteration temperature curves of wells CL4-A, CL5, CL6, and CL7

The present study analyses temperature data from the Cachaços-Lombadas wells in two ways. The formation temperature corresponds to the stabilized profiles taken in the wells after warm-up and the alteration temperature was assessed according to the occurrence and distribution of the secondary minerals. In this respect, a correlation between the formation and the alteration temperature curves is shown in Figure 30 which allows inferring the thermal evolution of the geothermal system.

The alteration temperatures from all wells are shifted to the right of the formation temperatures indicating that at some point in the past the geothermal system was slightly hotter, reaching temperatures up to 260°C. In the uppermost part of the reservoir down to 600 m depth, this shift is more pronounced in CL6 where the temperature difference is about 40-45°C while in the other wells the shift is only about 10 to 20°C. Additionally, the alteration temperature curves suggest that the geothermal system was shallower than today (about 50-100 m shallower at this location), suggesting that fluid levels within the geothermal system have been fluctuating with time.

The comparison of the alteration and formation temperatures indicates that cooling has occurred at some point in the past. During the binocular analyses, no significant evidence of retrograde alteration was found filling the open-spaces within the rock formations of the Cachaços-Lombadas wells. However, this does not exclude its presence. In this respect, it is important to note that the detailed petrography, performed in 2005 by the Foundation of the Science Faculty at the University of Lisbon, allowed to identify both retrograde and prograde alteration in thin sections from cutting samples of well CL6 (Figures 31 and 32) and these observations are consistent with the hypothesis that cooling has occurred at some point in the past.

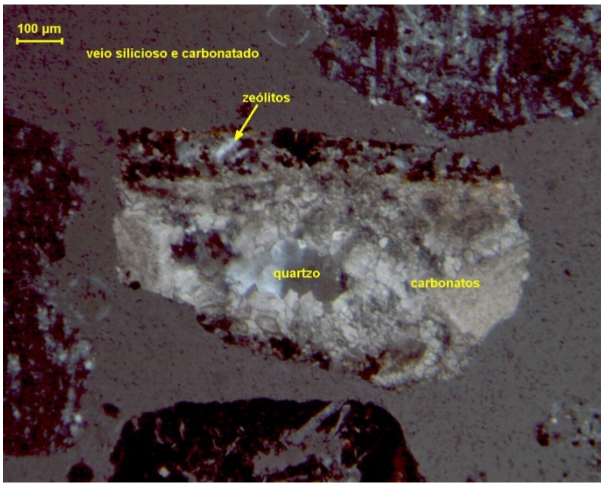

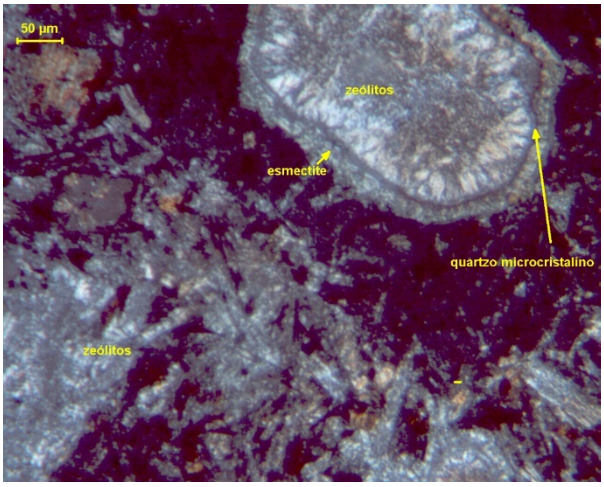

FIGURES 31 and 32: Samples from well CL6. In Figure 31 to the left, a vein is identified at 635 m composed of 1) zeolites, 2) calcite and 3) quartz, showing a prograde alteration. In Figure 32 to the right, a vesicle is identified at 542 m filled with 1) quartz, 2) smectite and 3) zeolites, showing retrograde alteration in a vesicle at CL6 (photos from Foundation of the Science Faculty at the University of Lisbon, 2005)

The investigation of the mineral sequences should be performed using detailed petrographic analysis and this was only executed thoroughly in well CL6 (CL5 only three samples were analysed). Therefore, the available data is not sufficiently conclusive regarding the existence of any retrograde or prograde alteration tendency and how these are distributed over the Cachaços-Lombadas area. Nevertheless, the rank of the alteration minerals, particularly the ones identified under the petrographic microscope in wells CL5 and CL6 such as prehnite, epidote and albite, suggest that the geothermal system was at slightly higher temperatures than the ones observed at present times.

The hypothesis that fluctuations of the reservoir fluid level have occurred in the past is more convincing (this is quite evident in CL5 and CL7) and is supported by the results from the fluid inclusion studies and by the observation of high abundance of calcite and quartz veins at about 0 to -150 m m.s.l. in most of the Cachaços-Lombadas wells.

10. CONCLUSIONS

All rocks intersected by the Cachaços-Lombadas wells are volcanic and correspond to the eruptive products of the Fogo volcano. The lithostratigraphy of the area can be summarized as follows:

- At shallow levels from the surface to about 250-300 m m.s.l. five wells intersect a thick sequence of trachyte lavas which are very permeable. This is the case of CL1, CL2, CL3, CL4 and CL4-

A. These trachyte lavas are absent in the wells CL5, CL6 and CL7, possibly because they thinned out or it were eroded in these locations;

- A thick sequence of pyroclastic rocks is the predominant lithology from the surface to about -100 m m.s.l. In CL5, CL6 and CL7 the sequence reaches about 600 m thickness but is thinner at CL4-A where it is 300-400 m thick. The sequence of pyroclastic rocks is locally interrupted by lava flows (mostly trachytes) of variable thickness. Here, four lava units have relatively good correlation between wells, working as marker horizons;
- The pyroclastic rock units show a progressive increase in the intensity of the hydrothermal alteration with depth, particularly to clay minerals which form the caprock of the geothermal system;
- Below sea level the subsurface geology is dominated by basalt lavas down up to about -600 m m.s.l. This is most prominent in CL4-A. Elsewhere, the extent of this lava dominated interval is rather uncertain, particularly in the area of wells CL6, CL5, and CL7 because this interval was drilled without returns;
- No intrusive or subvolcanic rocks were identified in the study but they may occur at greater depth;
- No pillow lavas were found in the depth interval logged down to -600 m m.s.l. This confirms the high rate of subsidence that the graben of Ribeira Grande has suffered.

The lithological data from the wells does not allow for direct identification of any faults. However, the location of the major permeable zones encountered in the Cachaços-Lombadas wells roughly coincide the NW and NNW trending inferred faults in the area, suggesting that the NNW trend structures may be associated with high permeability.

Boiling occurs in most of the wells, creating a two-phase or steam zone at the top of the reservoir. The only exception is well CL6, located further to the south, which only exhibits the liquid phase. Furthermore, the temperature distributions at 4 different elevations indicate:

- The temperature gradient is relatively high to about -100 m m.s.l. (in the range of 250-300°C/km);
- From -100 m m.s.l., the reservoir is near isothermal with temperatures ranging from 230-235°C in most parts of the area. This depth interval corresponds to the core of the geothermal reservoir where the most prolific feed zones are located;
- A slight temperature reversal is observed in the bottom part of most of the Cachaços-Lombadas wells, indicating that the main upflow zone of the geothermal system is not located in the central parts of the project development area of Cachaços-Lombadas;
- With increasing depth, the temperatures continue to increase towards NNE whereas in the southern part of the area the temperatures tend to decrease. This strongly indicates a boundary of the geothermal field in the south. Furthermore, the data are insufficient to locate precisely where the upflow zone is but the temperature distribution suggests that it may occur at some undetermined location to the east or northeast of CL3 and CL7.

The alteration mineral assemblage shows a trend where low temperature minerals like zeolites and opal form in the upper part of the wells and are gradually replaced by moderate temperature minerals like chalcedony and quartz which in turn give way to higher temperature minerals such as chlorite, prehnite, epidote and albite.

The occurrence and distribution of alteration minerals allowed the identification of two zones of hydrothermal alteration beneath a shallow zone of relatively unaltered rocks. A smectite zone (< 200-220°C) was identified from 150-200 to 500-590 m and a chlorite zone (> 230°C) below 500-590 m. Additionally, the alteration zoning pattern within the area indicated that higher alteration temperatures are found shallower in CL7 when compared to wells CL4-A, CL5, and CL6, suggesting that CL7 is closer to the upflow zone of the geothermal system.

Alteration temperatures, based in the first appearance of key index secondary minerals and in the homogenization temperatures of fluid inclusions, indicate that the geothermal system was hotter than today at some point in the past, with maximum temperatures up to 270-300°C, but it has been in equilibrium since then with some fluctuations of the fluid level in the reservoir.

Freezing studies carried out with fluid inclusions in quartz samples from CL7 confirmed that fresh water was the fluid of the geothermal system when the inclusions were trapped during the crystallization of the secondary quartz crystals and this is consistent with the composition of the reservoir fluid at the present time.

ACKNOWLEDGEMENTS

I wish to address my gratitude to the United Nations University – Geothermal Training Programme, in particular to Mr. Lúdvík S. Georgsson, director of the Geothermal Training Programme of the United Nations University (UNU-GTP) and to all the technical staff, namely Mr. Ingimar G. Haraldsson, Ms. Málfrídur Ómarsdóttir, Ms. Thórhildur Ísberg and Mr. Markús A.G. Wilde for their kind assistance and arrangements. These are extended to all the 2015 UNU fellows for their friendship and caring support during the training in Iceland. Special thanks to my fellow geologists Davar Ebrahimi, Frederick Mutua, Hamda Wais and Patrick Muanza for the continuous share of knowledge and ideas.

Sincere thanks to Dr. Björn S. Hardarson from ISOR for his advice and guidance during the development of this project. These are extended to Mr. Sigurdur Jónsson for the assistance in the X-ray diffraction analysis and to Dr Gunnlaugur Einarsson and Jóhann Kristjánsson from Orkustofnun for the support with the Petrel software. I am also thankful to Dr. Kristján Saemundsson for the valuable comments throughout the development of the project. A kind appreciation is also addressed to Professor Eniko Bali of the University of Reykjavik for the support during the fluid inclusion studies.

Finally, but not the last, a special word of appreciation is addressed to EDA Renováveis, S.A., for the support given during the training in Iceland and for allowing the use of the Ribeira Grande geothermal field data for the purpose of the present work.

REFERENCES

Booth, B., Croasdale, R., and Walker, G.P.L., 1978: A quantitative study of five thousand years of volcanism on São Miguel, Azores. *Royal Society of London Philosophical Transactions, 288*, 271-319.

Cabeças, R., Carvalho, J., Nunes, J., 2010: Portugal country geothermal update 2010. *Proceedings of the World Geothermal Congress 2010, Bali, Indonesia*, 10 pp.

Carmo, R., 2013: *Neotectonic studies in São Miguel Island, a contribution for the study of seismic risk in the Azores.* PhD dissertation in Geology, specialty in Volcanology (in Portuguese). Department of Geoscience, University of the Azores, 307 pp.

Carvalho, M., Forjaz, V., Almeida, C., 2006: Chemical composition of deep hydrothermal fluids in the Ribeira Grande geothermal field (São Miguel, Azores). *J. Volcanology and Geothermal Research, 156*, 116–134.

Carvalho, A., Sousa, M., Oliveira, C., Campos-Costa, A., Nunes, J., and Forjaz, V., 2001: Seismic hazard for the central group of the Azores Islands. *Boll.Geofisica Teorica ed Applicata, 42-1/2*, 89-105.

Cole, P., Queiroz, G., Wallenstein, N., Gaspar, J., Duncan, A., and Guest, J., 1995: An historic subplinian/phreatomagmatic eruption: the 1630 AD eruption of Furnas volcano, São Miguel, Azores. *J. Volcanology and Geothermal Research, 69*, 117-135.

Dawson, P., Silva, A., Lyerl, H., and Evans, J., 1985: Seismic study of the Agua de Pau geothermal prospect, São Miguel, Azores. *Geothermal Resources Council Transactions, 9*, 401-406.

Duffield, W.A., and Muffler, L.J.P., 1984: *Geothermal resources of São Miguel Island, Azores, Portugal*. U.S. Geological Survey, open-file report 84–287, 21 pp.

EDA – Electricidade dos Açores, 2014: *Demand and offer of electricity (in Portuguese).* Electricidade dos Açores (EDA), Planning, Control of manageament and regulation (PLCOR), Ponta Delgada, São Miguel, Azores, Portugal, 32 pp.

Ferreira, T., 2000: *Characterization of the volcanic activity in São Miguel Island (Azores), recent basaltic volcanism and degassing areas. Risk assessment.* PhD dissertation (in Portuguese), Geoscience Department, University of Azores, 248.

Foundation of the Science Faculty at the University of Lisbon, 2005: *Petrographic and diffractometric characterization of selected samples from wells CL5 and CL6, Ribeira Grande geothermal field (in Portuguese)*. University of Lisbon, report for Sociedade Geotérmica dos Acores, S.A. (SOGEO), 22.

Gaspar, J.L., 1996: *Graciosa Island (Azores), volcanological history and assessment of hazards.* University of the Azores, Azores, PhD dissertation (in Portuguese), 256 pp.

GeothermEx, 2008: *Update of the conceptual and numerical model of the Ribeira Grande geothermal reservoir, São Miguel, Açores*. GeothermEx Inc., report for Sociedade Geotérmica dos Açores, S.A. (SOGEO), 190 pp.

GeothermEx, 2014: *Selection of new drilling sites in the Cachaços-Lombadas sector, Ribeira Grande geothermal field, São Miguel, Açores*. GeothermEx Inc., report for EDA Renováveis, 46 pp.

Granados, E., Hennerberger, R., Klein, C., Sanyal, S., Ponte, C., Forjaz, V., 2000: Development of injection capacity for the expansion of the Ribeira Grande geothermal project, São Miguel, Açores, Portugal. *Proceedings of the World Geothermal Congress 2010, Kyushu-Tohoku, Japan*, 3065-3070.

Hennerberger, R., and Nunes, J., 1990: A new discovery well in the upper Água de Pau geothermal system, São Miguel Island, Azores: results of drilling and testing. *Geothermal Resources Council Transactions, 14*, 1449-1452.

Irvine, T.N., and Barager, W.R.A., 1971: A guide to the chemical classification of the common volcanic rocks. *Canadian Journal of Earth Sciences, 8*, 523-548.

Madureira, P., Moreira, M., Mata, J., and Alle`gre, C., 2005: Primitive neon isotopes in Terceira Island (Azores archipelago). *Earth and Planetary Science Letters, 233*, 429–440.

Madureira, P., Moreira, M., Mata, J., Nunes, J., Gautheron, C., Lourenco, N., Carvalho, R. and Abreu, M., 2014: Helium isotope systematics in the vicinity of the Azores triple junction: constraints on the Azores geodynamics. *Chemical Geology, 372*, 62–71.

McGraw, P., 1976: *A petrological/geochemical study of rocks from the São Miguel drillhole, São Miguel, Azores.* MSc dissertation, University of Dalhousie, 194 pp.

Métrich, N., Zanon, V., Créon, L., Hildenbrand, A., Moreira, M., and Marques F., 2014: Is the 'Azores hotspot' a wetspot? Insights from the geochemistry of fluid and melt inclusions in olivine of pico basalts. *Journal of Petrology, 55*, 377–393.

Moore, R., 1990: Volcanic geology and eruption frequency, São Miguel, Azores. *Bulletin of Volcanology, 52*, 602–614.

Moore, R., 1991: Geology of three late Quaternary stratovolcanoes on São Miguel, Azores. *US Geological Survey Bullettin 1990*, 46 pp.

Muecke, G., Ade-Hall, J., Aumento, F., MacDonald, A., Reynolds, P., Hyndman, R., Quintina, J., Opdyke, N., and Lowrie, W., 1974: Deep drilling in an active geothermal area in the Azores. *Nature, 252*, 281-285.

Pham, M., Klein, C., Ponte, C., Cabeças, R., Martins, R., and Rangel, G., 2010: Production/injection optimization using numerical modeling at Ribeira Grande, São Miguel, Azores, Portugal. *Proceedings of the World Geothermal Congress 2010, Bali, Indonesia*, 6 pp.

Ponte, C, 2012: Case study – Use of geothermal resources for power production in the Azores (in Portuguese). *Ingenium magazine, September/October edition*, 67-67.

Ponte, C., Cabecas, R., Rangel, G., Martins, R., Klein, C., Pham, M., 2010: Conceptual modelling and tracer testing at Ribeira Grande, São Miguel, Azores, Portugal. *Proceedings of the World Geothermal Congress, Bali, Indonesia*, 11 pp.

Ponte, C., Cabeças, R., Martins, R., Rangel, G., Pham, M., and Klein, C., 2009: Numerical modeling for resource management at Ribeira Grande, São Miguel, Azores, Portugal. *Geothermal Resources Council Transactions, 33*, 847-853.

Queiroz, G., 1997: *Sete Cidades volcano (São Miguel Island, Azores) – eruptive history and hazard assessment.* PhD dissertation (in Portuguese), University of the Azores, 226 pp.

Rangel, G., Franco, A., Cabeças, R., Ponte, C., 2011: Use of geothermal resources in the Azores Islands: A contribution to the energy self-sufficiency of a remote and isolated region. *Geothermal Resources Council Transactions, 35*, 1209-1214.

Rangel, M.G., 2014: Temperature model and tracer test analysis for the Ribeira Grande geothermal system, São Miguel Island, Azores. Report 29 in: *Geothermal training in Iceland 2014*. UNU-GTP, Iceland, 615-642.

Rodrigues, M, and Oliveira, C., 2013: Seismic zones for Azores based on statistical criteria. *Natural Hazards Earth System Sciences, 13*, 2337–2351.

Silva, R., 2011: *Evaluation of spatial and temporal seismicity patterns in the central region of São Miguel (Azores): implications for whole-island seismic hazard assessment*. University of the Azores, PhD dissertation, 236 pp.

Walker, G., and Croasdale, R., 1970: Two Plinian-type eruptions in the Azores. *J. Geological Society of London, 27*, 17-55.

Wallenstein, N., Duncan, A., Chester, D., and Marques, R., 2007: Fogo volcano (São Miguel, Azores): a hazardous edifice. *Géomorphologie: Relief, Processes, Environment, 3*, 259-270.

APPENDIX I: Detailed description of the lithological units of wells CL4-A, CL5, CL6, AND CL7

CL4-A

Well CL4-A was drilled to 1076.4 m during June 3 and July 26, 2012. The 13-3/8´´ production casing was set at 613.5 m and the 9-5/8´´ slotted liner was installed at 1,067.4 m, hanging at 588.4 m depth inside the production casing (note: all depths correspond to total measured depths from the ground floor level). The lithological units intersected by the well can be summarized as follows:

0-24 m: *Pyroclastic deposits*. Three pyroclastic units can be distinguished, with a tuff rich scoria at the top, followed by lithic tuff and a pumice bed at the bottom.

24-182 m: *Trachyte lava*. White to light grey, hard, porphyritic with sanidine phenocrysts. Locally it is slightly vesicular. Common oxide stains in the felsic groundmass which peak at 174 m. From 124 m loose sanidine crystals are abundant. This could be the same sequence of lava found in CL1 and CL2, located in the southern part of Cachaços-Lombadas sector, or some separate but similar sequence of lava.

182-230 m: *Lithic tuff*. The formation is brownish grey and poorly consolidated. Matrix of ash, tan to brownish grey, partially altered to clay. Lithics of mostly fresh lava, exhibiting oxidation. The first appearance of calcite is at 196 m. Opal and chalcedony are common as open space fillings, mainly as amygdales in the lithics of vesicular lava which are found in minor quantities.

230-340 m: *Basalt lava*. Dark brownish grey, moderately consolidated. The lava is pervasively altered to clay, vesicular, with light grey-green to white fillings likely microcrystalline quartz or chalcedony. The groundmass is mottled by clay alteration (mainly smectite). At 238 m sulphur crystals were found, suggesting that at same point in the past this corresponded to an open permeable zone, likely a fracture through which steam was circulating onwards from 270 m the first veins of quartz and calcite appear. The lava in the uppermost part of this interval seems to be decomposed, possibly by weathering prior to burial.

340-360 m: *Lithic tuff*. Brown to brownish grey, poorly consolidated. Matrix of ash is altered to brownish clay (mainly smectite). Lithics of different lavas: dark grey basalt lava, fine-grained, locally with replacements and veins of calcite + quartz; light grey to grey lava, porphyritic with feldspar phenocrysts, moderately hard to soft, pervasively altered to clay and with oxide spots. Minor reddish-orange lava, strongly oxidized and silicified and greenish grey lava with abundant amygdales filled with smectite + opal, with the groundmass mottled by clay alteration.

360-380 m: *Trachyte lava*. The lava flow sequence is light grey to brownish grey, moderately hard, porphyritic with sparse hyaline feldspar phenocrysts (sanidine). At the top it is vesicular with white opal fillings/coatings, locally with calcite + quartz replacements.

380-480 m: *Lithic tuff*. The deposit is grey to brownish grey, poorly consolidated to moderately consolidated. Matrix of ash altered to clay, was mostly washed away during drilling, appears as coatings on the lava lithics. Lithics of dark grey to brownish grey lava, porphyritic with sanidine phenocrysts, locally with chlorite + quartz replacements and with calcite + quartz + hematite veins. Common lithics of light grey lava and reddish brown lava, strongly oxidized, as well as light grey vesicular lava with white to white green fillings. Minor syenite fragments and loose quartz, the latter probably from open-space fillings (veins). Weak to moderately altered, mostly clay (likely smectite), calcite (veins, veinlets and replacements), silica (quartz veins and replacements, and opal fillings). Chlorite appearance is at 450 m, becoming more common with increasing depth.

480-510: *Basalt lava*. The lava flow sequence is grey to dark grey, compact, hard, with calcite + quartz veinlets and veins, locally associated with chlorite. Common loose quartz + calcite, likely from open space fillings (veins). Additionally, locally the lava exhibits patchy hematite. Weak to moderately altered, mainly calcite, quartz, chlorite and hematite.

10-624 m: *Lithic tuff*. The pyroclastic deposits are brownish grey to grey, poorly consolidated. Matrix of ash has been mostly washed away but is locally indurated by silicification, related to the deposition of microcrystalline quartz or chalcedony. Lithics of mostly grey to brownish grey lava, with abundant calcite + chlorite replacements, strongly oxidized. Minor lithics of light grey lava with opal fillings, the groundmass mottled by clay alteration. Locally with very fine pyrite at 564 m. Common loose quartz + chlorite, probably from open-space fillings (veins) which are very abundant at the top (510-516 m). At 582 m found amygdales filled with calcite + quartz + chlorite. Calcite is abundant in the whole interval. Moderately altered.

624-896 m: *Basalt lava*. Dark grey, hard, aphanitic to locally porphyritic with pyroxene phenocrysts, locally with quartz + calcite replacements, veins and veinlets (all locally associated with chlorite and pyrite). Occasionally, the pyroxene phenocrysts exhibit oxide staining. The groundmass is relatively fresh, fine grained but locally is chloritized at 688-702 m. Minor presence of white altered rock, silicified, with very fine disseminated pyrite, appears at 682 m and at 700-724 m. Oxidation peaks up at 702 m and the same occurs with the white open space fillings (quartz and quartz + calcite. Red jasper is found locally at 724 m and the chlorite replacements peak at 724 m.

896-900 m: *Trachyte lava*. The lava is white to light grey, moderately hard, fine grained, with calcite + chlorite replacements, locally with very fine cubic pyrite.

900-914 m: *Basalt lava*. Dark grey, moderately hard, fine grained, with calcite + quartz replacements, locally with patchy hematite. Minor loose calcite + quartz from open-space fillings with most of the crystals being hyaline.

914-1010 m: *Intermmediate lava*. The lava is grey to light grey, moderately hard. Fine grained, aphanitic. Calcite is less abundant than above. Common loose white and hyaline crystals mostly quartz and quartz + calcite, from open-space fillings (veins). Locally with fine disseminated pyrite and with hematite stains.

1010-1083 m: *No information*. Drilled without returns.

CL5

Well CL5 was drilled to 1,132.0 m during October 31, 1999 to January 31, 2000. The 13-3/8′′ production casing was set at 613.5 m and the 9-5/8′′ slotted liner was installed at 1,067.4 m, hanging at 588.4 m depth inside the production casing. The lithological units intersected by the well can be summarized as follows:

0-288 m: *Pyroclastic rock units*. Relatively unconsolidated pyroclastics rock units (mostly lithic tuffs and pumice deposits) dominate from surface to about 288 m. Light grey to tan pumice beds are found at 110-120 m and interlayered with lithic tuff from 151-170 m.

288-345 m: *Trachyte lava*. Light grey, moderately hard to hard. Consists at least of two flow units separated at 315-320 where there is a brown clay matrix and minor weathering of some of the lava. Overall, the lava is massive, fine grained with sugary appearance. Sparse phenocrysts of sanidine and rarely amphibole can be seen. Unaltered to weakly altered, only locally some hematite on weathered surfaces (310-320 m).

345-515 m: *Pyroclastic rock units*. This interval may contain several units but the most prominent are the lithic tuff units found at 345-390 and 400-445 m which are interlayered with two main tuff units, a consolidated tuff from 390-400 m which seems to be indurated by silicification, and at the bottom from 445 to 515 m the ash matrix is overall altered to clay and silicified with common very fine disseminated pyrite. A scoria unit is found at 445-555 m.

515-540 m: *Basalt lava*. The lava flow sequence is grey to brownish grey, hard, fine grained. Weakly to moderately altered, with partial replacements of calcite, chalcedony and possibly zeolite veins. First appearance of chlorite is at 525 m and it becomes common down to the bottom of the well.

540-615 m: *Lithic tuff.* The lithics of lava make up from 20 to 70%. Veins of chalcedony, quartz, chlorite, pyrite and occasionally hematite are common.

615-645 m: *Basalt lava*. Dark grey to grey, hard, massive, fine grained. The lava is pervasively altered, with abundant calcite replacements and locally with patchy chlorite. Hematite is locally intense. Veins are common, in various assemblages, such as calcite + quartz, quartz + pyrite, quartz + pyrite + chlorite, calcite + chlorite.

645-655 m: *Lava breccia*. The formation is red to grey, corresponding to a breccia zone between two lava flows. Alteration is strong to moderate, mostly calcite + chlorite, some silicification and hematite.

655-697 m: *Basalt lava*. The lava flow sequence is dark grey to grey, hard, massive and fine-grained. Mostly is pervasively altered, with abundant calcite and chlorite replacing the groundmass minerals.

Veining is locally abundant, mainly quartz + chlorite + pyrite + calcite and rarely quartz + pyrite + hematite.

697-703 m: *Tuff*. White to tan, moderately consolidated. Pervasively silicified. The tuff is replaced by chalcedony and chlorite. Very fine disseminated pyrite is abundant. Veining is rare.

703-1076 m: *No information*. Drilled without returns.

CL6

Well CL6 was drilled to 1,239.2 m between January 26th and April 27th, 2005. The 13-3/8´´ production casing was set at 719.8 m and the 9-5/8´´ slotted liner was installed at 1,227 m, hanging at 693 m depth inside the production casing. The lithological units intersected by the well can be summarized as follows:

0-135 m: *Lithic tuff, lithic-pumice tuff and pumice beds*. Poorly consolidated to unconsolidated pyroclastic deposits are predominant with the intersection of several tuff and lithic tuff units from the surface to a depth of 270 m. Two pumice beds are found at 21-25 m and 91-93 m and from 34 to 44 m there is a crystal rich tuff with abundant loose crystals of sanidine.

135-188 m: *Lithic tuff*. The formation is grey to yellow-brown, poorly to moderately consolidated. Matrix of ash partially altered to tan, white and yellow clay (mostly likely smectite), contains also very fine silte to sand size crystals and lithics. Lithics of compact grey lava, porphyritic with sanidine phenocrysts, locally vesicular with white clay fillings. Minor loose crystals of sanidine and grey to yellow-orange pumice, the latter making up to 5-10%. Rare volcanic glass. Scoria bed is present at 136-140 m.

188-270 m: *Lithic tuff*. The formation is grey-green, moderately consolidated. Matrix of tan to light greenish grey ash, containing very fine silt size crystals, altered to clay (possibly smectite and minor chlorite), locally indurated by silification. Lithics of grey, light grey and grey-green compact lava, often oxidized. Some lava lithics are vesicular, with tan to yellow fillings (likely smectite and zeolites). Rare syenite fragments.

270-327 m: *Trachyte lava*. Light grey to white, moderately hard to hard, fine grained, massive, porphyritic with sanidine phenocrysts, locally exhibiting oxide stains. Locally the lava is soft where it is decomposed to clay. At 285 m abundant pyrite clusters were found associated with microcrystalline quartz. Additionally, yellow sulphur was found at 285 to 291 m, suggesting the possibility that some fault/fracture is or was present in that zone through which steam is or was flowing. The logging team at drilling site did not identify the sulphur crystals, but reported that samples had a strong sulphur smell. Note also that this is possibly the same trachyte unit encountered from 288-345 m in CL5. The different depths of intersection in the two wells suggest that this lava dips northward or north westward which is consistent with the structure of the Fogo volcano. Also important to note is that near the top of this trachyte lava there is a zone of stronger mineralization with clusters of pyrite, calcite and quartz. This zone does not occur in CL5, suggesting that the mineralization may be associated with a specific fracture zone passing through the lava. This is consistent with the sulphur crystals reported above.

327-400 m –*Lithic tuff and pumice-lithic tuff*. The formation is light grey to tan, moderately consolidated. Matrix of white to tan ash, partially altered to clay, comes up mainly as clusters and as coatings on the lithics but locally is also indurated by silicification. Lithics of light grey to dark grey lava, porphyritic with sanidine phenocrysts. Grey pumice is not found much in the whole interval but is dominant at 333 m, suggesting that a pumice bed could had been deposited here.

420-448 m - *Trachyte lava*. The lava is light grey to light brownish grey, moderately hard, with abundant oxide stains, fine grained, porphyritic with sanidine phenocrysts.

448-500 m – *Lithic tuff and crystal-lithic tuff.* The formation is light grey to brown and purple, poorly to well consolidated. Matrix of ash altered to white to grey clay, mostly washed away during drilling but appears as coatings on the lithics. Lithics of lava include trachyte and basalt types, some scoria and minor altered rock.

500-581 m – *Lithic tuff.* The formation is dark grey to brownish and purple grey. Matrix of ash altered to brown clay (mainly smectite). Lithics of mostly grey to dark grey lava, fine-grained, porphyritic with sparse sanidine phenocrysts, locally with calcite replacements. Minor lithics of trachyte lava and volcanic glass. Common loose feldspar and loose silica fragments (likely microcrystalline quartz or chalcedony), the later from open space fillings (veins and veinlets). The lava lithics exhibit common oxide staining. At 541 m vesicular lithics of lava with chalcedony amygdales were found. It is noticeably that the amount of the silica veins increases with depth.

581-620 m - *Basalt lava*. The lava sequence is dark grey, moderately hard, fine grained, with common calcite + quartz replacements, veins and veinlets (locally associated with chlorite). The interval has abundant white to hyaline loose crystals, from open space fillings (veins and veinlets), mainly corresponding to quartz and quartz + calcite. Moderately altered, mainly open space fillings and replacements of silica, calcite. The groundmass is locally chloritized onward from 587 m.

620-668 m – *Lithic tuff.* The formation is dark grey to brownish grey. Matrix of brown to red-brown altered ash, altered to clay and moderately indurated by silicification from the deposition of microcrystalline quartz. Lithics of mostly basalt lava, dark grey, aphanitic, vesicular with calcite + quartz and quartz fillings, locally plus chlorite with hematite on the rims. Clear calcite and quartz crystals are relatively common and loose microcrystalline quartz + calcite crystals are relatively abundant.

668-680 m - *Basalt lava.* The lava is dark grey, aphanitic, fine-grained, with quartz + calcite + chlorite replacements. Abundant white to white green open space fillings from amygdales, veins and veinlets. Common silica eggs likely quartz. Moderately altered, mainly clay, silica, chlorite and iron oxides.

680-710 m - *Lithic tuff.* The formation is variable coloured, dark grey, dark brown and light brown-green, moderately consolidated. Matrix of dark brown to light brown clay, locally indurated by silicification. Lithics of grey to blue-green, grey and dark grey lavas with common calcite + quartz replacements (locally plus chlorite). Moderately altered, mainly clay, calcite, silica, chlorite and iron oxides.

710-811 m - *Basalt lava*. The lava is dark grey, hard to moderately hard, porphyritic with olivine and sparse pyroxene phenocrysts. This appears to be a relatively continuous sequence with only minor breaks, caused by brecciation between lava flows. Hyaline and white loose crystals are relatively abundant from open-space fillings (veins and veinlets) with the most common assemblages found being quartz, quartz + calcite and quartz + calcite + chlorite, locally with hematite (abundant at 716 m). From 750 m the lava sequence is weakly chloritized but the chloritization peaks and is intense below 787 m. Rare occurrence of red jaspe, likely from veins. According to the detailed petrographic analysis, prehnite is also occasionally present, often associated with calcite. Additionally, at 775 m growing aureoles of secondary albite were found around the plagioclase phenocrysts.

811-910 m - *Altered rock.* The formation is white to greenish grey, moderately hard, pervasively altered to silica and chlorite. The alteration obscures the original lithology of the formation but relict textures suggest that at least part of this sequence may be pyroclastic. In this interval, calcite is common but its intensity is significantly weaker than above. The cuttings become very fine below 826 m, making it even more difficulty to identify the rock type. The rock is overall silicified and with very fine disseminated pyrite. XRD and detailed petrographic analysis revealed that there is abundant zeolite within the rock fragments (probably laumontite or wairakite) as well as secondary albite. The appearance of epidote is at 823 m.

910-1239 m – No information. Drilled without returns.

CL7

Well CL7 was drilled to 1,166 m between February 27 and April 8, 2010. The 13-3/8´´ production casing was set at 599 m and the 9-5/8´´ slotted liner was installed at 1,147 m, hanging at 567 m depth inside the production casing. The lithological units intersected by the well can be summarized as follows:

0-120 m: *Pyroclastic rock units*. The deposits include lithic tuff, crystal-pumice tuff and pumice beds. Variable amounts of loose crystals of sanidine are found in this interval but they are abundant at 40-46 m. Two pumice beds are found in this interval at 26-36 m and 104-108 m.

120-270 m: *Lithic tuff*. Light grey to light greenish grey, poorly to moderately consolidated. Matrix of ash altered to white and light grey clay (mostly smectite, coexisting with kaolinite at the top and from 200 m with illite), locally silicified likely due to the deposition of opal and/or chalcedony. Lithics of mostly light grey trachyte lava. Clay alteration peaks at 126 m and silicification is stronger below 240 m. Pyrite appears at 110 m and quartz appears at 234 m.

270-308 m: *Trachyte lava*. White to light greenish grey, moderately soft, mostly altered to clay and locally indurated by silicification. Common fine disseminated pyrite.

308-384 m: *Pyroclastic rock units*. Two lithic tuff units are present at 308-366 m and 370-384 m, interrupted by a thin basalt lava flow at 366-370 m. The tuff is pervasively altered to white and white-green clay (mainly illite, coexisting with chlorite at the bottom of the interval) and is weakly to strongly silicified, locally with patchy chlorite. The lithics of lava are mostly of basaltic composition, with calcite + quartz replacements.

384-416 m: *Trachyte lava*. Light grey, fine-grained, compact, with quartz replacements. The alteration is more intense in the top of the interval in the less dense part of the lava flow. This sequence differs from the trachyte lavas commonly found in geothermal field, as the sanidine phenocrysts that are often present in these type of lavas are not evidently present in this section, possibly eroded due to alteration.

416-500 m: *Lithic tuff*. The formation is light grey to grey, moderately consolidated. Matrix of ash is pervasively altered to white and light greenish grey clay, indurated by silification and locally chloritized. Lithics are mostly trachyte lava. Common loose quartz, quartz + calcite crystals whose abundance peaks at 464 and at 476 m; additionally, loose pyrite is abundant in the whole interval.

500-522 m: *Trachyte lava*. The lava is light grey to white, moderately hard, fine-grained, with sugary appearance, locally with feldspar phenocrysts being replaced by clay, hematite and quartz.

522-588 m: *Pyroclastic rock units*. At least two lithic tuff deposits are found in this interval. The ash matrix is overall silicified and chloritized. The lithics of lava are predominantly of basalt with common quartz + calcite veinlets and replacements.

588-596 m *Basalt lava*. Dark grey, hard, aphanitic, with calcite + quartz replacements and patchy hematite. Locally chloritized.

596-620 m: *Lithic tuff*. Moderately consolidated, this unit is more homogeneous than the pyroclastic units found above from 522-588 m.

620-1173 m: No information, drilled without returns.

APPENDIX II: Lithology logs of wells CL4-A, CL5, CL6, and CL7

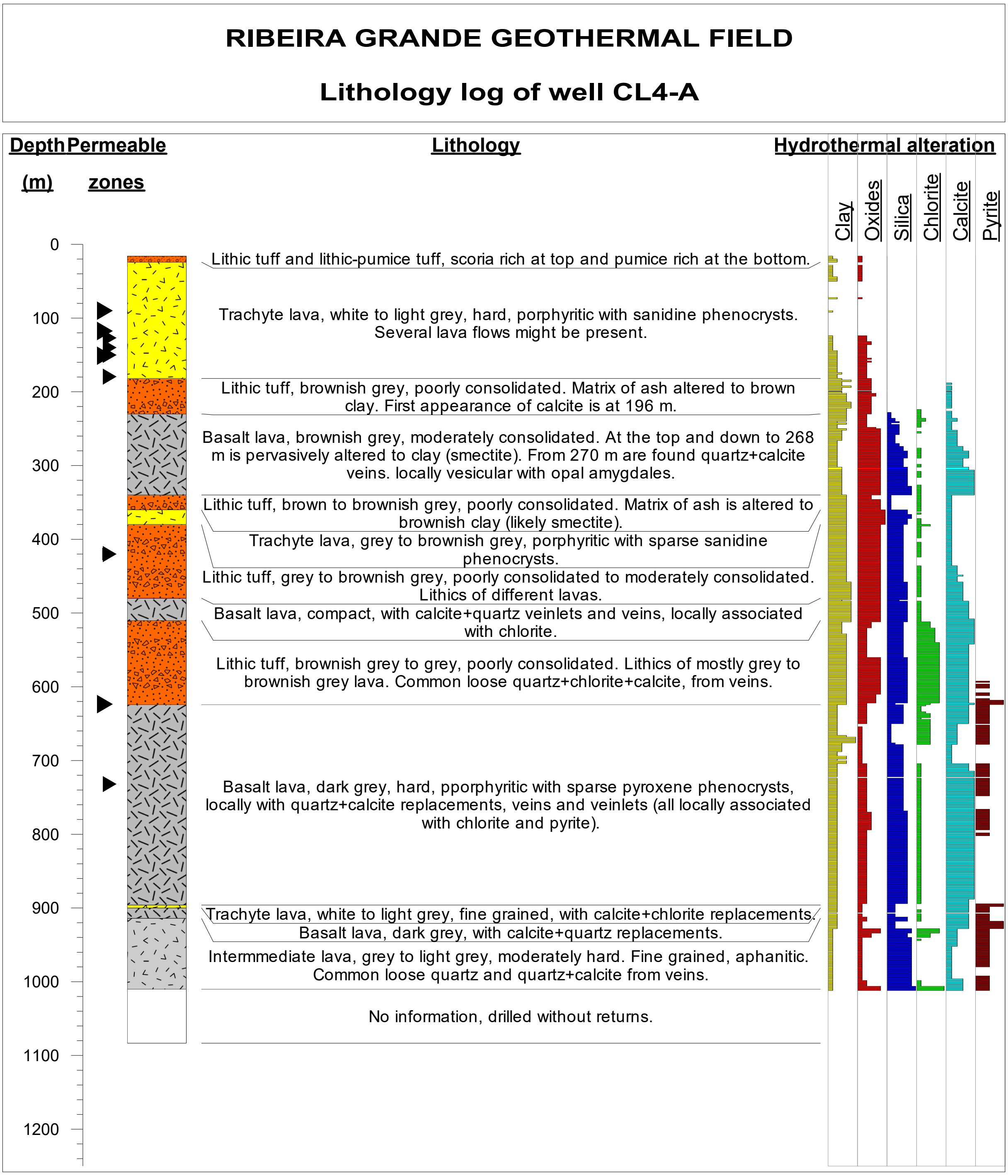

Company Name: EDA RENOVÁVEIS, S.A.
Drilling Contractor: Iceland Drilling; Drilling rig: Jotunn
Drilling dates: June 3 - July 26, 2012; Total drilling time = 56 days
Well Coordinates (UTM WGS 84 - Zone 26N):
East = 632.872 m; North = 4.183.047 m; Elevation = 441 m Drilled depth = 1173 m

RIBEIRA GRANDE GEOTHERMAL FIELD

Lithology log and alteration zones of well CL5

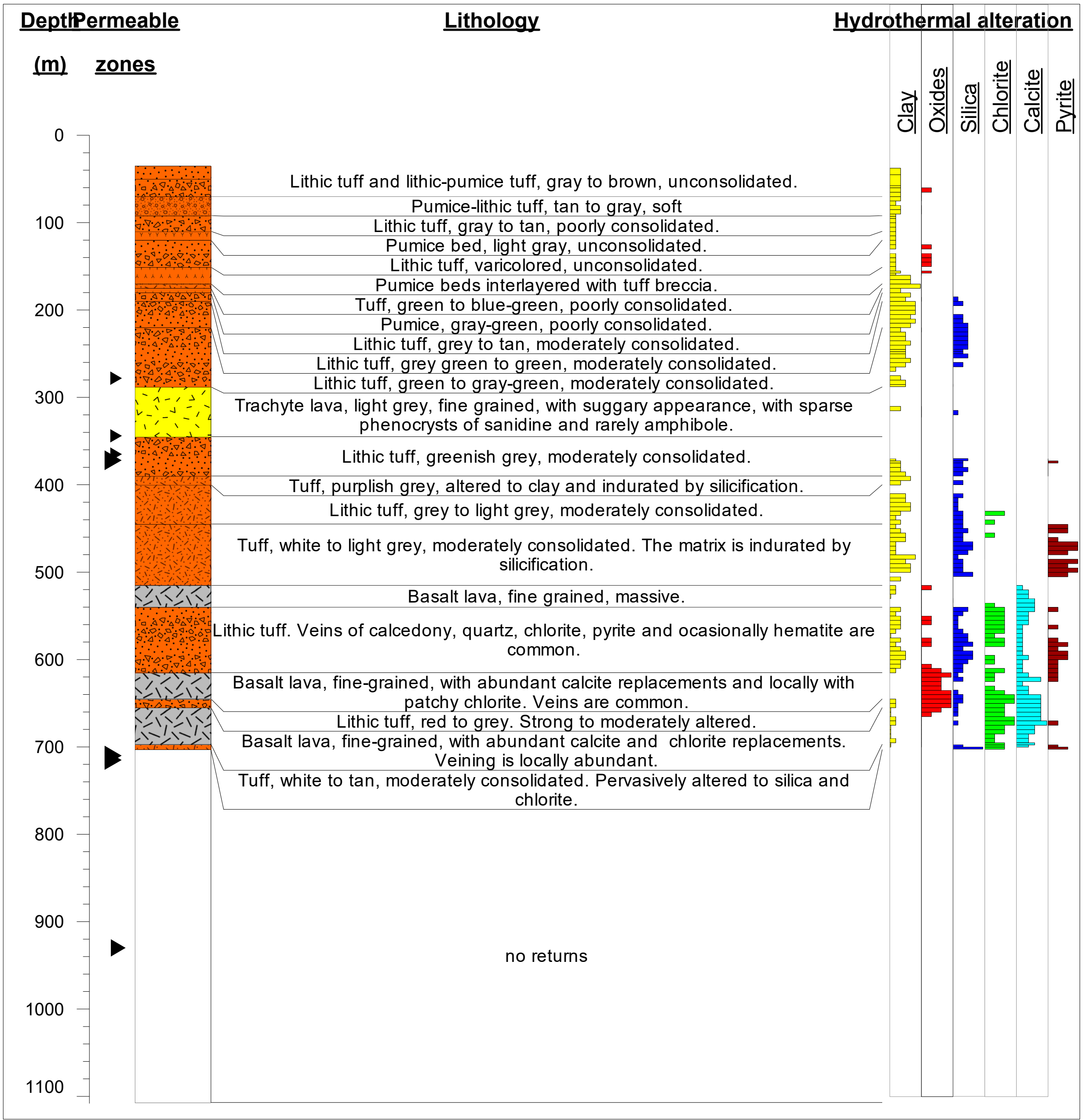

Company Name: EDA RENOVÁVEIS, S.A.
Drilling Contractor: Iceland Drilling; Drilling rig: Jotunn
Drilling dates: Oct, 31st, 1999 to Jan, 17th, 2000; Total drilling time = 62,0 days
Well Coordinates (UTM WGS 84 - Zone 26N):
East = 633.028,2 m; North = 4.182.428,20 m; Elevation = 495,0 m Drilled depth = 1.139,0 m

RIBEIRA GRANDE GEOTHERMAL FIELD

Lithology log of well CL6

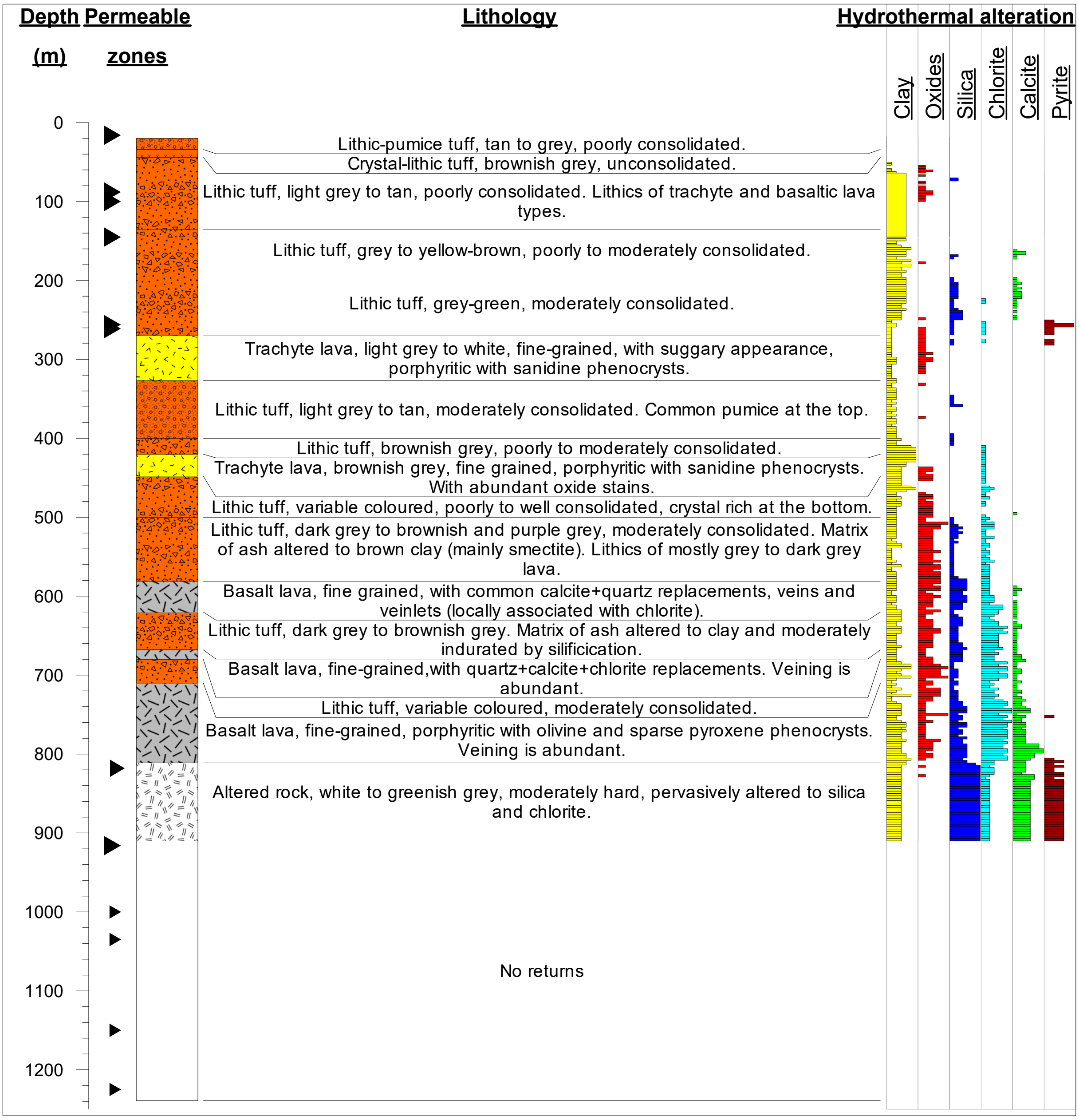

Company Name: EDA RENOVÁVEIS, S.A.
Drilling Contractor: Iceland Drilling; Drilling rig: Ingerssol Rand RD20 (1st stage. from 0 to 135 m); Jotunn
Drilling dates: January, 26th to April, 27th, 2005; Total time for operations = 54 days
Well Coordinates (UTM WGS 84 - Zone 26N):
East = 633.048,9 m; North = 4.182.402,50 m; Elevation = 503.5 m Drilled depth = 1239.2 m

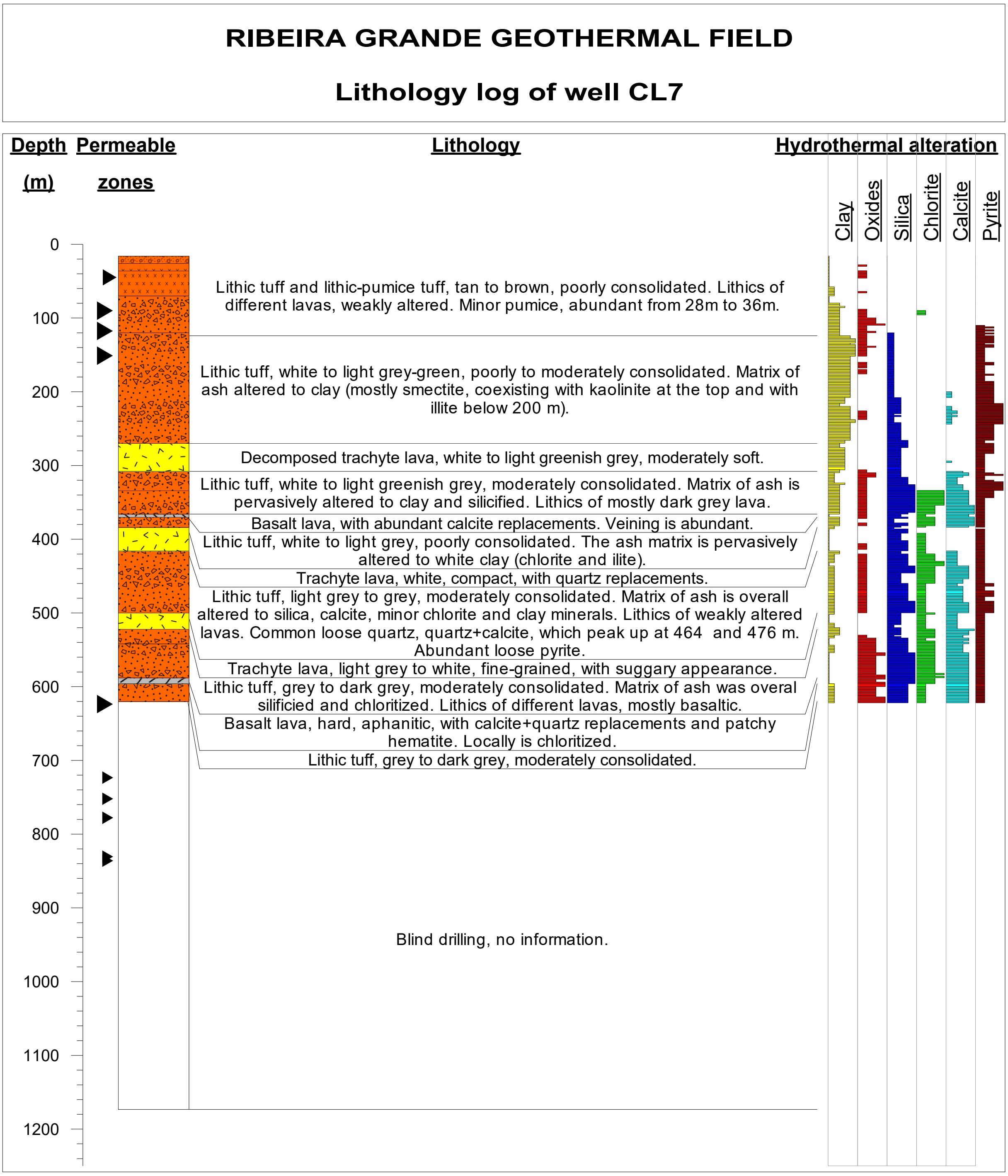

Company Name: EDA RENOVÁVEIS, S.A.
Drilling Contractor: Iceland Drilling; Drilling rig: Jotunn
Drilling dates: February 27 - April 8, 2010; Total time for operations = 40 days
Well Coordinates (UTM WGS 84 - Zone 26N):
East = 633.024 m; North = 4.182.605 m; Elevation = 487 m Drilled depth = 1173 m

APPENDIX III: Formation temperature profiles of wells CL1, CL2, CL3, CL4, CL4-A, CL5, CL6, CL7, and CL8

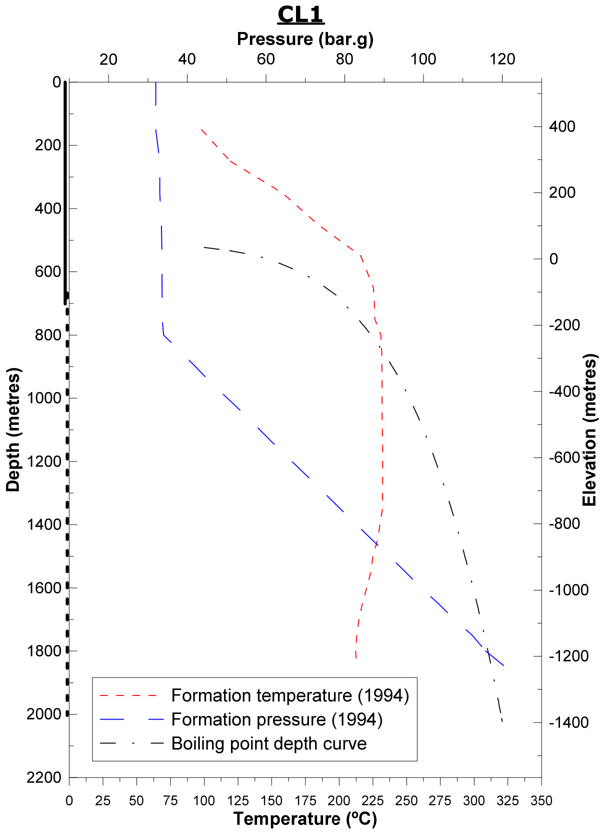

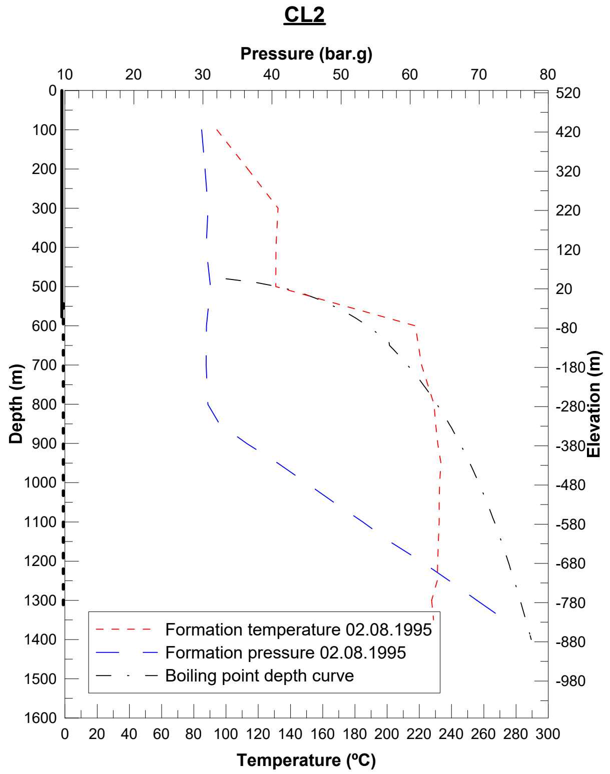

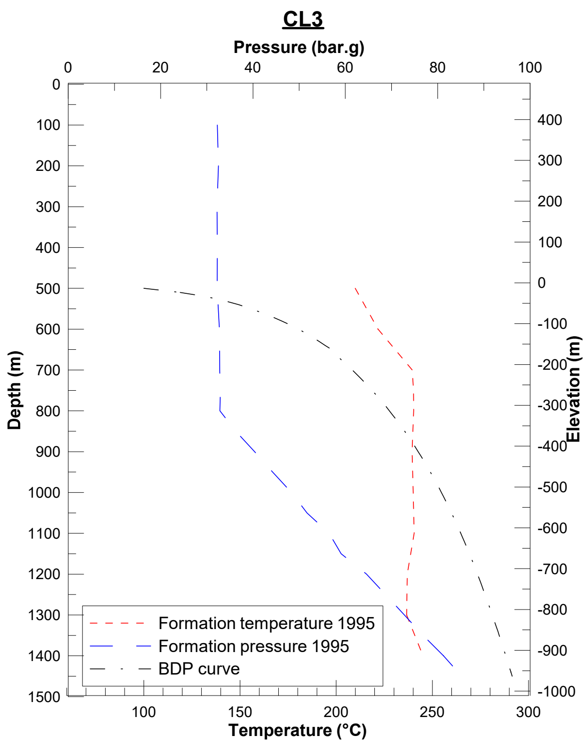

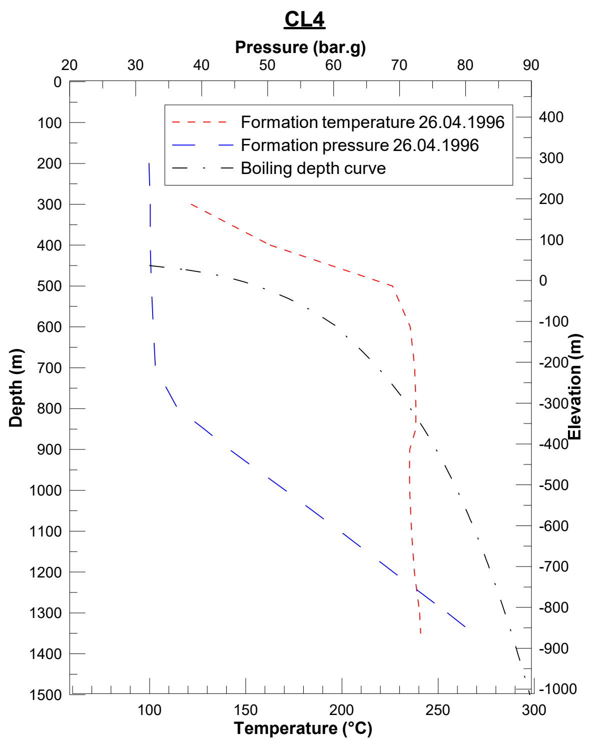

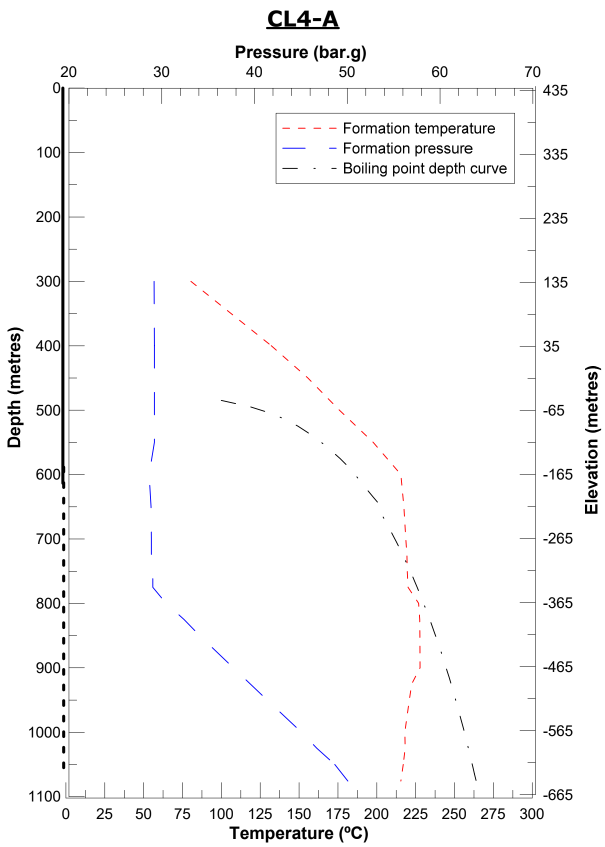
CL4-A
Pressure (bar.g)
Formation temperature
Formation pressure
Boiling point depth curve
Depth (metres)
Elevation (metres)
Temperature (ºC)

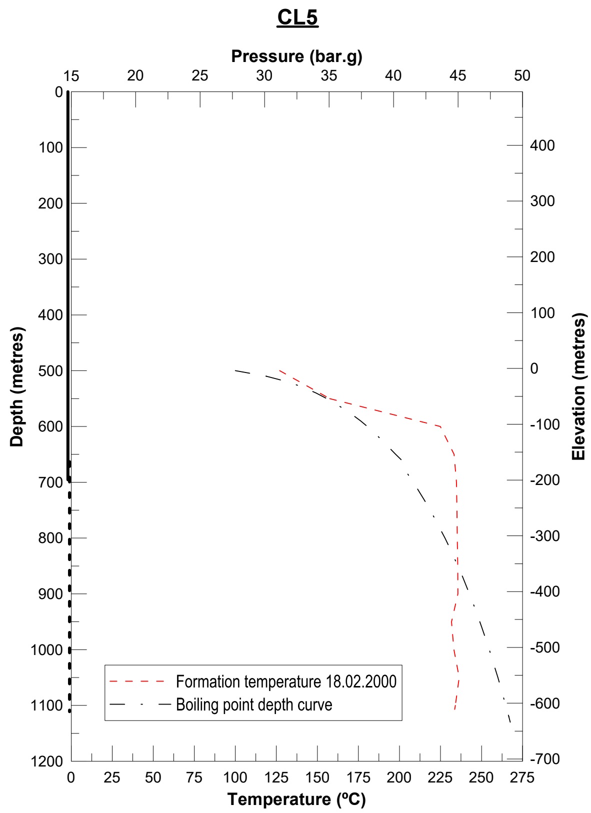
CL5
Pressure (bar.g)
Formation temperature 18.02.2000
Boiling point depth curve
Depth (metres)
Elevation (metres)
Temperature (ºC)

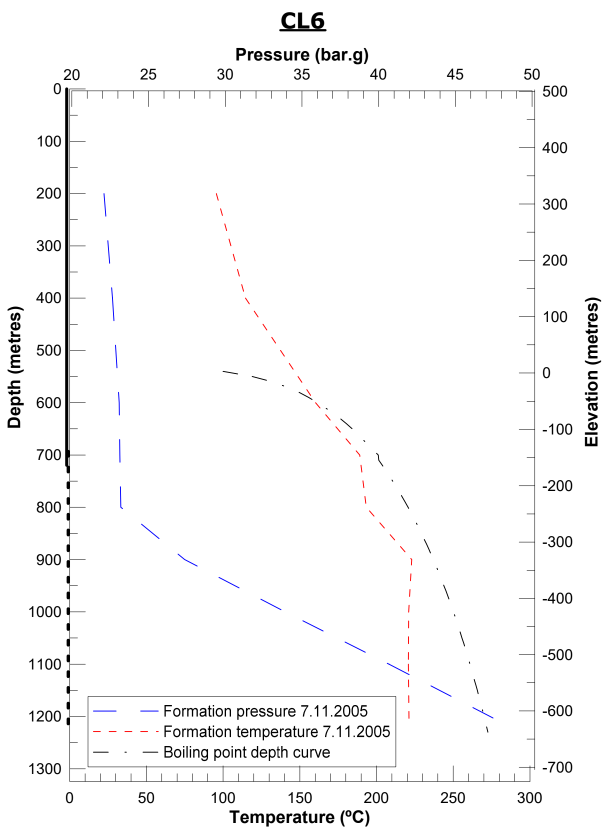
CL6
Pressure (bar.g)
Formation pressure 7.11.2005
Formation temperature 7.11.2005
Boiling point depth curve
Depth (metres)
Elevation (metres)
Temperature (ºC)

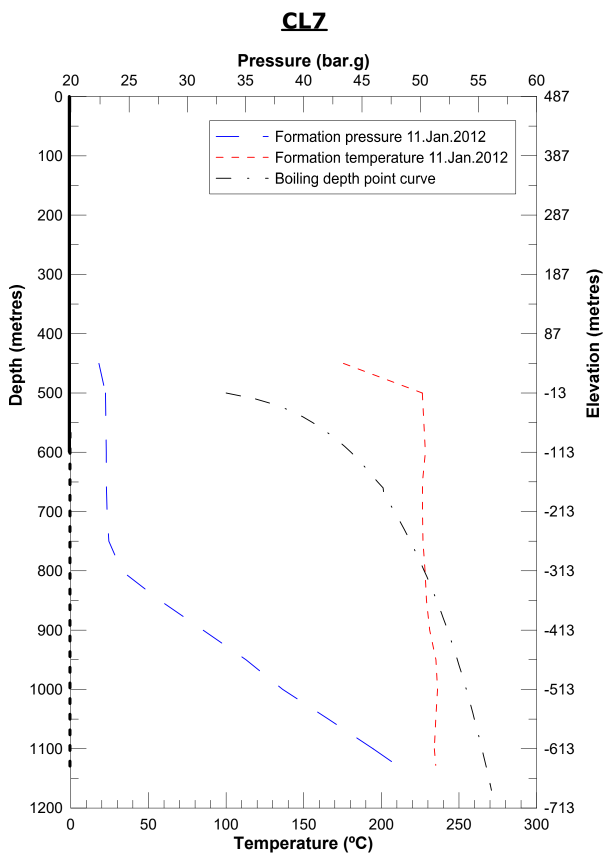
CL7
Pressure (bar.g)
Formation pressure 11.Jan.2012
Formation temperature 11.Jan.2012
Boiling depth point curve
Depth (metres)
Elevation (metres)
Temperature (ºC)

APPENDIX III: X-ray diffractometry results from wells CL4-A, CL5, CL6, and CL7

X-ray diffractometry analyzis conducted at ISOR laboratory (2015)

Well	Depth (m)	Untreated (Å)	Glycolated (Å)	Heated (Å)	Minerals identified
CL4-A	236	n.d.	n.d.	n.d.	no clays
CL4-A	280	13.02	14.22	10.08	Smectite
CL4-A	348-350	13.02	14.22	10.13	Smectite
CL4-A	450-452	10.94/7.21	10.94/7.21	10.29/n.d.	Kaolinite. Ilite is probably present but there is a odd shift in the heated peak.
CL4-A	550-552	14.83/10.03	14.83/10.03	7.24/10.03	Chlorite and minor traces of ilite
CL4-A	638	14.62/10.14	14.62/10.14	7.24/10.14	Chlorite. Ilite might be present, but the fact that the heated peak is higher than the untreated is kinda odd.
CL4-A	730-732	12.86/7.20	14.05/7.02	9.96/n.d.	Smectite. Minor traces of kaolinite
CL4-A	934	14.71/10.58	14.71/10.58	7.2/10.58	Chlorite + Ilite
CL4-A	836	14.69/10.30	14.69/10.30	7.22/10.30	Chlorite and minor traces of ilite
CL4-A	1008	14.37	14.37	7.14	Unstable chlorite
CL5	170-175	n.d.	n.d.	n.d.	no clay
CL5	220-250	6.62	6.62	6.62	no clay. Traces of some type of feldspar.
CL5	345-390	12.37/6.58	13.51/6.58	10.11/6.58	Smectite. Traces of some type of feldspar
CL5	490-495	6.59	6.59	6.59	No clay. Traces of some type of feldspar
CL5	525	n.d.	n.d.	n.d.	no clay
CL5	590-605	14.34/14.34	14.3/14.34	13.99/7.20	Unstable chlorite
CL5	655	14.34/14.34/10.23/6.43	14.34/14.34/10.23/6.43	14.34/7.18/10.23/6.43	Unstable chlorite. Minor traces of ilite and some type of feldspar
CL5	705	17.48/11.46	17.48/11.46	n.d.	Residual peaks at 17 and 11A, but no positive identification
CL7	140-148	17.48/7.32	17.48/7.32	10.26/n.d	Smectite + kaolinite
CL7	198	13.75/6049	15.65/6.49	10.01/6.49	Smectite. Traces of some type of feldspar
CL7	234	10.38	10.38	10.38	Possibly ilite, but there is a rather weird heated peak, which is higher than the glyco and untreated peaks (these are very low, almost absent)
CL7	280-286	10.53	10.53	10.53	Ilite
CL7	380	14.52/10.79	14.52/10.79	7.31/10.79	Chlorite + Ilite, almost equally abundant.
CL7	448-452	14.34/12.80	14.34/13.15	7.24/10.07	Chlorite coexisting with smectite (not MLC), almost equally abundant.
CL7	540	14.54/14.54	14.54/14.54	7.18/10.07	Chlorite + smectite, equally abundant.
CL7	560	14.45/12.78	14.45/13.38	7.18/10.03	Chlorite+Smectite, with chlorite more abundant.
CL7	614	14.32/10.03	14.32/10.03	7.18/10.03	Chlorite and minor ilite

n.d. = no difraction

X-ray diffractometry analyzis conducted at Faculdade de Ciencias da Universidade de Lisboa (2005)

Well	Depth (m)	Untreated (Å)	Glycolated (Å)	Heated (Å)	Minerals identified
CL6	217	n.a.	n.a.	n.a.	Sanidine, Clorite and ilite
CL6	397	n.a.	n.a.	n.a.	Sanidine, quartz and ilite
CL6	415	n.a.	n.a.	n.a.	Sanidine and ilite
CL6	563	n.a.	n.a.	n.a.	Sanidine, quartz and ilite
CL6	704	n.a.	n.a.	n.a.	Quartz, sanidine, hematite and ilite
CL6	727	n.a.	n.a.	n.a.	quartz, hematite, albite and chlorite (nimite)
CL6	793	n.a.	n.a.	n.a.	Quartz, hematite, chlorite (nimite) and ilite (?)
CL6	814	n.a.	n.a.	n.a.	quartz, albite, Chlorite and ilite
CL6	910	n.a.	n.a.	n.a.	Quartz, ortoclase, albite and traces of ilite
CL5	703	n.a.	n.a.	n.a.	Albite, quartz and chlorite

n.a. = not available